Chapter 4

THE REFLEX EXOSKELETON

Hemiparetic gait is characterized by strong asymmetries that can severely affect the quality of life of stroke survivors. This asymmetry is due to motor deficits in the paretic leg and the resulting compensations in the non-paretic limb. By actively promoting gait symmetry in hemiparetic patients, the necessity of these compensations should be reduced and, therefore, motion changes should be detected in both paretic and non-paretic lower limbs.

This chapter presents the design and preliminary validation of the REFLEX prototype, a unilateral active Knee-Ankle-Foot Orthosis able to naturally assist the paretic limb of hemiparetic patients during gait. Results proved the feasibility of REFLEX to assist gait by reinforcing symmetry. They also pointed out that the assistance of the paretic leg decreased the compensatory strategies developed by the non-paretic limb to achieve a functional gait.

4.1 Introduction

Asymmetric gait in hemiparetic patients is due to misfunctions in the paretic leg (such as motor weakness, or control or proprioceptive loss [328]) but also due to compensation mechanisms developed in the non-paretic limb. Despite physical therapy, which can improve gait speed and endurance of hemiparetic subjects, asymmetric gait can be resistant to intervention [36] and is still present in 50% of community-dwelling chronic stroke patients [275].

In this context, where motor recovery after stroke remains a clinical challenge [208], robotic exoskeletons have been presented not only as rehabilitation tools [143] but also as assistive devices for hemiparetic subjects. As detailed previously in this document (see section 1.4), several authors have developed partial robotic exoskeletons to improve

post-stroke gait quality, demonstrating the feasibility of robotic assistance to hemiparetic gait. However, there is still a lack of understanding about how these subjects react to this assistance and if they are able to integrate the robot's action and adapt their gait pattern accordingly.

In this chapter, the robotic exoskeleton REFLEX (symmetRy-rEinForcer uniLateral powEred eXoskeleton) is presented as a tool to investigate these adaptation processes and the effect of unilateral gait assistance on hemiparetic subjects. This device was designed to promote post-stroke gait symmetry by guiding the paretic knee movement during the swing phase and reinforcing this joint during the stance phase, which was previously reported to be a successful assistive target [236, 388]. In this framework, the control paradigm defined in chapter 3 is used to assist the subject's gait, according to the *Echo* (section 3.3.1) and *Pattern* (section 3.3.2) strategies.

The REFLEX's overall objective is to enable the intuitive control of the device, which would lead to the improvement of the technology embodiment through a natural interaction between the user and the robotic exoskeleton. This proper and natural interaction between these two systems will enable the patients to consider the robot's action as a part of their own gait capability, improving their gait quality as a consequence [209]. If the robot action, which counteracts gait impairments, is integrated into the neural gait control, compensatory strategies would be reduced since they arose to deal with such impairments. Thus, the REFLEX prototype is a tool to assess the subject's adaptation to the exoskeleton's assistance and evaluate the effects of the human-robot interaction in both paretic and non-paretic legs.

4.2 The REFLEX prototype

The REFLEX prototype is a Knee-Ankle-Foot orthosis (KAFO) composed of two joints aligned to the knee and ankle of the user (figure 4.1). The segments' length and the braces' positions can be tailored to the anthropometry of different users. The material of the major part of the prototype is aluminum 7075, so the result is a robust and lightweight device. The total weight of the KAFO is approximately 4kg.

The REFLEX design is based on the robotic exoskeleton prototypes previously developed by the Neural and Cognitive Engineering Group from CSIC [28, 44, 293]. The knee joint is actuated by a DC EC-60 flat 408057 brushless motor (Maxon ag, Switzerland) coupled with a CSD-20-160-2AGR harmonic drive (Harmonic Drive LLC, EE.UU.). The transmission ratio of 1:60 of this system enables the application of a mean torque of 35 Nm. The ankle joint of the prototype remains non-actuated and unlimited, enabling its free movement in the sagittal plane. The prototype is equipped with four sets of

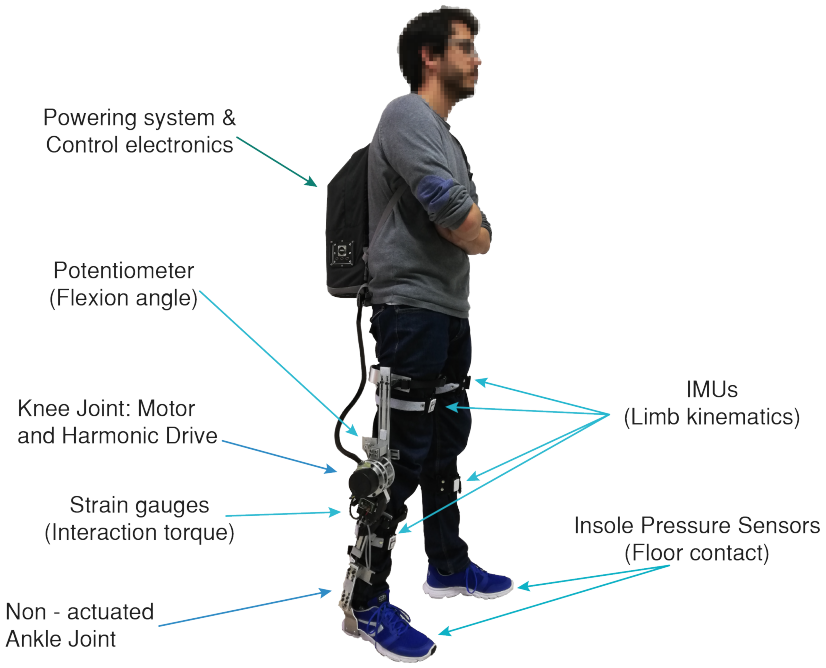

FIGURE 4.1: REFLEX prototype for the assistance of the knee joint of the paretic leg. This joint is actuated by a DC motor coupled to a Harmonic Drive, while the ankle remains unactuated. The sensors of the prototype are a potentiometer to measure the exoskeleton flexion in the sagittal plane, strain gauges to measure the interaction torque, inertial sensors (IMUs) to acquire the limbs kinematics, and insole pressure sensors to detect floor contact events.

sensors that provide information on system variables that are used in real-time control algorithms:

1. A potentiometer, coupled with the knee joint axis, was used to measure the flexion/extension angle of the active joint. This information enables the robot to follow trajectories using a closed-loop position control algorithm.

2. An interaction torque sensor was placed between the robot and the user. It consists of two pairs of strain gauges in a full Wheatstone bridge. This interaction torque is used to implement an impedance controller that adjusts the torque provided by the robotic system to the user's leg.

3. Three insole pressure sensors based on FSRs (Force Sensing Resistors) were used to assess the contact of each user's foot with the floor. Their measurements distinguish between swing and stance phases and adapt the controllers accordingly.

4. Four inertial measurement units (IMUs) (TechMCS, Technaid, Spain) were used to compute the kinematics of both legs. These sensors were attached to both legs' shanks and thighs to measure the flexion/extension angles of the hips and knees.

The control electronics of the prototype is composed of several dedicated modules and a main microcontroller; a schematic representation of the control architecture is shown

in figure 4.2. The control system is based on the *LaunchXL F28377S* board (Texas Instrument, USA), which runs the main control algorithm and communicates with the rest of modules that compose the system. A dedicated subsystem acquires the user's gait data based on the *Nucleo F446RE* board (STMicroelectronics, USA). Both boards are connected through a Controller Area Network (CAN) bus to send and receive information packages.

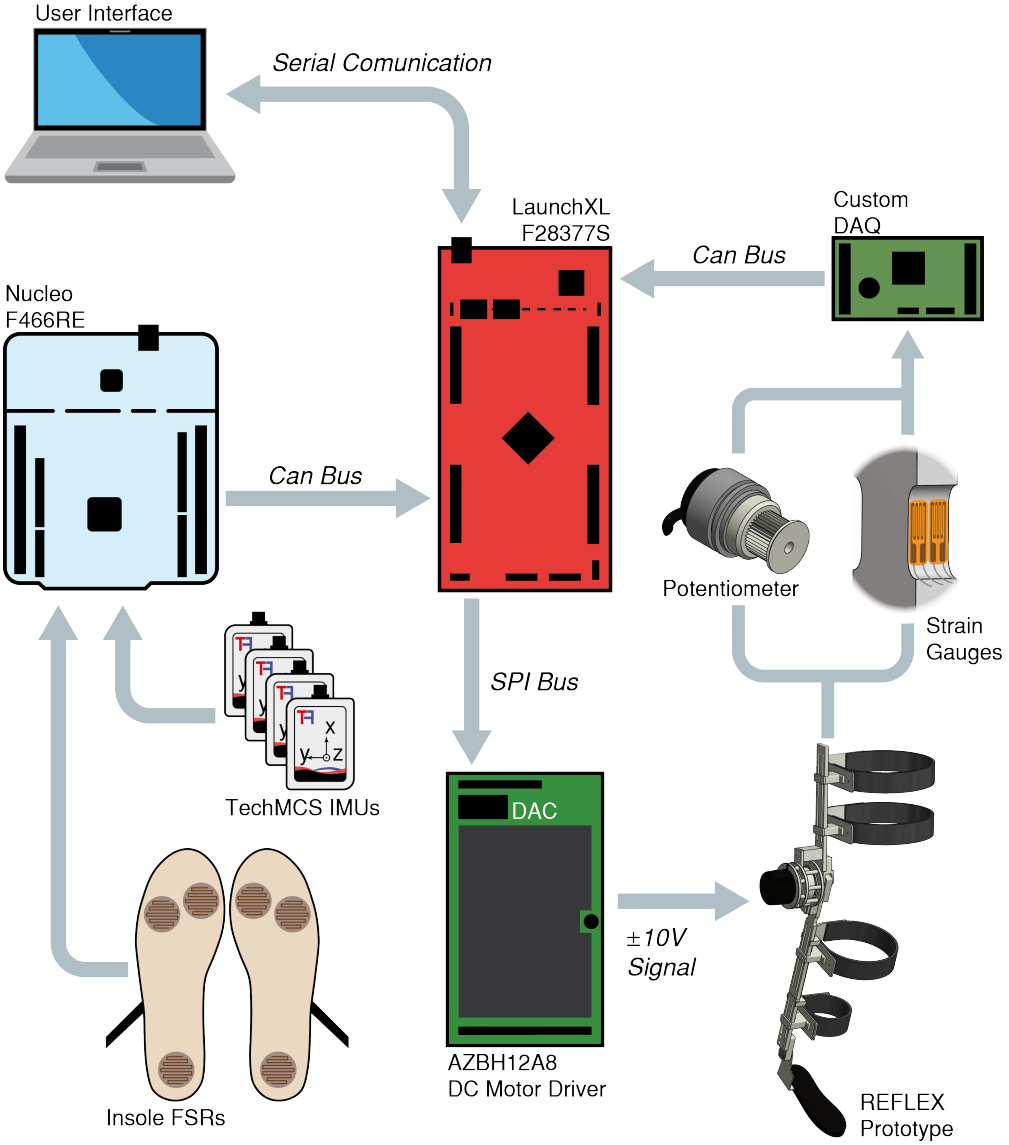

FIGURE 4.2: Control architecture of the REFLEX prototype. The main controller runs in the *LaunchXL* board that communicates with the rest of the modules. The DC motor of the prototype is commanded by the *AZBH12A8* driver by using a DAC managed by the main microcontroller through an SPI bus. Meanwhile, a custom DAQ measures the embedded sensors of the prototype (a potentiometer and four strain gauges) and sends this information to the main microcontroller through a CAN bus. The user's gait data is acquired by the *Nucleo* board from four *TechMCS* IMUs and three insole pressure sensors at each foot; this information is sent to the main microcontroller through a CAN bus. The full system is controlled using a user interface that runs on a laptop that communicates with the main microcontroller through a Serial bus.

An *AZBH12A8* driver (Advanced Motion Controlled, USA) is used to command the REFLEX's actuator. The required analog control signal is generated by a Digital-Analog Converter (DAC) commanded by the main microcontroller through a Serial Peripheral Interface (SPI) bus. A custom Data Acquisition System (DAQ) based on a *dsPIC30F4011* microcontroller (MicroChip Technology Inc., USA) is responsible for reading the information from the potentiometer (angular position) and the strain gauges (interaction torque) of the device. A CAN bus communicates this DAQ with the main microcontroller.

The main microcontroller also connects with a user interface through a Serial connection. In this interface, the researcher or the therapist can configure several parameters and record data from experiments. The sample frequency of the control algorithms, actuator, and DAQ acquisition is 1 kHz; however, the sample frequency of gait data (IMUs and FSR) and data logging in the user interface is 50 Hz.

The system can be used in a tethered version or a portable set-up where the exoskeleton's control electronics and a Li-Po battery are embedded in a backpack that is carried by the user. In this case, the power and electronic system's total weight is approximately 3 kg.

4.3 REFLEX control paradigm

Following the biomimetic control paradigm presented by Tucker et al. [357], the REFLEX controller is organized in a hierarchical structure composed of three layers (see figure 4.3).

1. In human gait, the volitional control originates in the supraspinal or cortical level, where the visual and vestibular information is integrated to modulate the generated gait patterns [86]. Analogously, the high-level control of the REFLEX prototype commands the global system and sets some parameters for the lower-level controllers. This high-level controller is implemented in the user interface and allows to start and stop the robot action and configure some parameters such as the assistance level.

2. Human gait locomotor patterns are generated at the spinal level by the CPG [99]. At this level, afferent information from muscle spindles, Golgi tendon organs, or tactile mechanoreceptors is also integrated to adapt the generated pattern [287]. Similarly, kinetic and kinematic gait patterns are generated in the middle-level controller to act as reference for the robotic devices. This controller should also be adaptive to the current gait state to tailor the generated reference. In the REFLEX prototype, the implemented middle-level controllers were the previously proposed

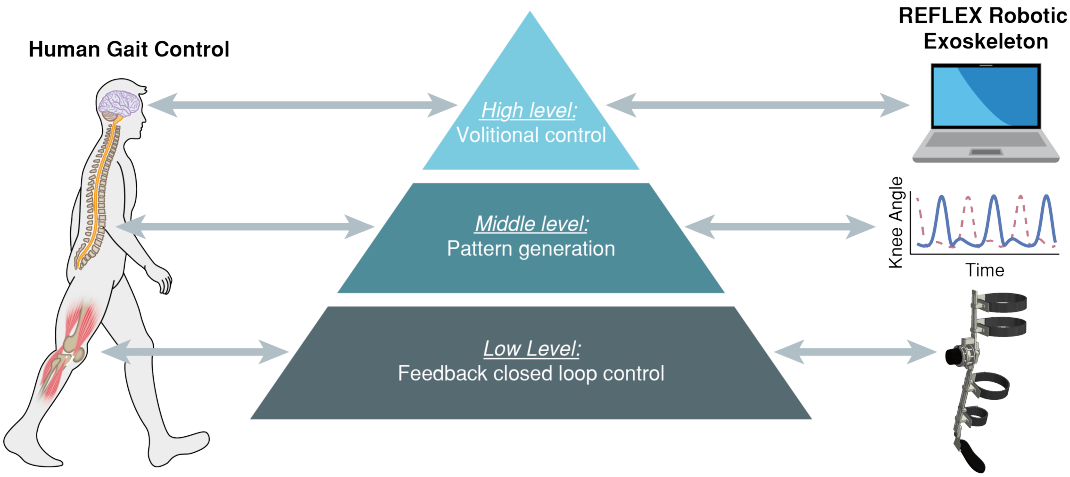

FIGURE 4.3: Biomimetic approach for controlling the REFLEX prototype. The high-level controller, implemented through the user interface, is responsible for the volitional control and corresponds with the supraspinal gait control. The pattern generation is the middle-level controller and corresponds with the CPG at the spinal level. In the lowest level, the controller is responsible for closing the feedback loop and performing the movement by managing the REFLEX's actuator, analogously to the recruitment of the lower limb muscles.

in chapter 3, i.e., the *Echo* control (see section 3.3.1), and the *Adaptive Healthy Pattern* control (see section 3.3.2)

3. Eventually, the locomotor pattern is performed by the muscles recruited by the efferent nerves to contract them according to the generated patterns. Afferent pathways transmit sensory information from the musculoskeletal system, closing the feedback loop for human gait control [357]. Likewise, the low-level control of a robotic exoskeleton is responsible for closing the control loop to track references and reject disturbances. In this regard, the REFLEX prototype implements an impedance controller to adjust the interaction torque between the exoskeleton and the user accordingly to the deviation from the kinematic pattern generated by the mid-level controller.

4.3.1 Variable impedance low-level controller

The assistance provided by the exoskeleton is based on a variable impedance model that aims at controlling the interaction between the robot and the user [144]. The mechanical impedance of a system ($Z(s)$) is defined as the relation between the force exerted by such a system against an external movement and the movement itself. In biomechanics, this impedance is defined as the relation between joint torque ($\tau(s)$) and movement ($\theta(s)$) [188], as depicted in the next equation:

$$Z(s) = \frac{\tau(s)}{\theta(s)} = I \cdot s^2 + B \cdot s + K \tag{4.1}$$

thus:

$$\tau(t) = I \cdot \ddot{\theta} + B \cdot \dot{\theta} + K \cdot \theta \tag{4.2}$$

According to equations 4.1 and 4.2, an impedance model allows to tailor the exerted torque according to angular, velocity and acceleration values (θ, $\dot{\theta}$ and $\ddot{\theta}$ respectively) depending on three components, namely: stiffness (K), damping (B), and inertia (I).

As in previous related works [178, 236, 379], the impedance controller has a twofold objective depending on the current gait phase (see figure 4.4):

1. During the stance phase, the robot aims to reinforce the limb so that the system composed of the leg and the exoskeleton can load the user's weight and not collapse. A high-impedance model is responsible for this reinforcement since it avoids substantial deviations from the prescribed kinematic pattern.

2. During the swing phase, the robot guides the limb's movement according to the Assisted-As-Needed (AAN) paradigm. The computed error between the reference kinematics and the actual movement serves as the input for the impedance model that defines the torque applied by the device to assist the user's gait. No torque is applied if the error is null, while higher errors imply higher assistive torques. The impedance model depends on the assistance level selected by the therapist or the user, so the force tunnel around the desired trajectory can be changed according to the user's needs.

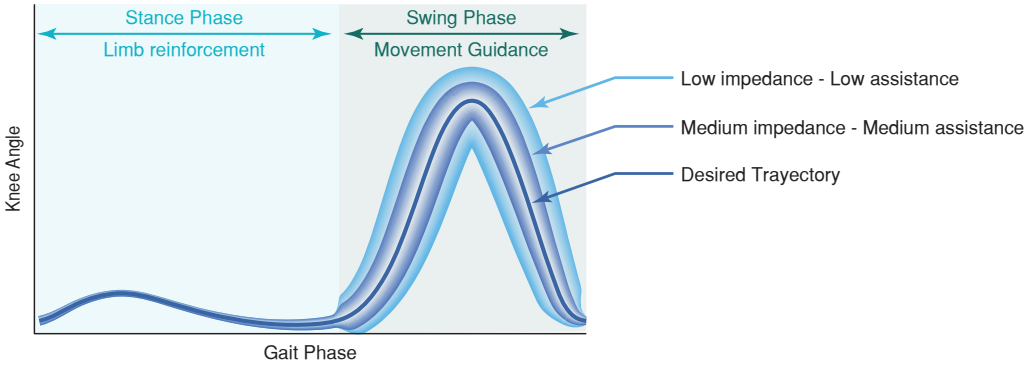

FIGURE 4.4: Force tunnel around the desired trajectory. The two assistance strategies used during a single step are represented: the exoskeleton reinforces the joint during the stance phase while it guides the movement during the swing phase; following the AAN paradigm, the exoskeleton is able to provide different assistance levels by using different force tunnels as depicted in the image.

According to the force-tunnel paradigm, the impedance model calculates the interaction torque that the exoskeleton should provide due to the angular reference tracking error. The system uses a PID controller to follow this torque interaction reference and provide it to the user (figure 4.5).

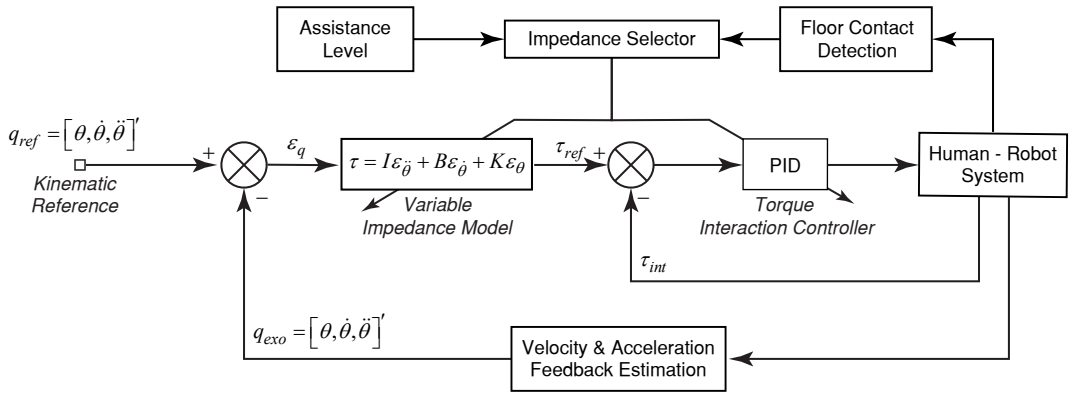

FIGURE 4.5: Low-level controller of the REFLEX. The block diagram represents the variable impedance controller; this controller assists the knee movement following the kinematic reference and according to an AAN paradigm.

As previously mentioned, the correct timing for the provided assistance is a critical factor for the embodiment of the REFLEX prototype. In this sense, the low-level controller needs to reduce as much as possible the delays between the prescribed and actual movement of the device, maintaining a stable behavior. Properly defining the impedance model allows for compensating the damping and inertia of the robotic system, allowing the device to track the motion reference with lower delays.

The velocity and acceleration reference patterns generated by the middle controller are used to implement this compensation. The error between these patterns and the measured joint velocity and acceleration are inputs of the impedance model to calculate the corresponding interaction torque. Instead of calculating the velocity and acceleration signals directly from angular measurements, a Kalman filter is used to overcome the highly noisy result of discrete derivatives (figure 4.6, panel A). The system model used in this Kalman filter was identified using experimental data from the REFLEX's joint. The panel B of figure 4.6 shows an example of the resulting signals after using the Kalman filter; as can be seen, the noise in the filtered signals is reduced, especially in the acceleration feedback, without introducing any appreciable delay.

Figure 4.7 compares the performance of the original exoskeleton controller, based only on angular feedback and described in [28], with the new controller that includes velocity and acceleration feedback. As it can be seen, the REFLEX's controller substantially reduces tracking errors and delays, which are especially important for the proper embodiment of the device (details in table 4.1). Statistical analysis of tracking errors and delays in the instant of maximum knee flexion proved the better performance of the REFLEX controller (Mann-Whitney U test, $P < 0.005$).

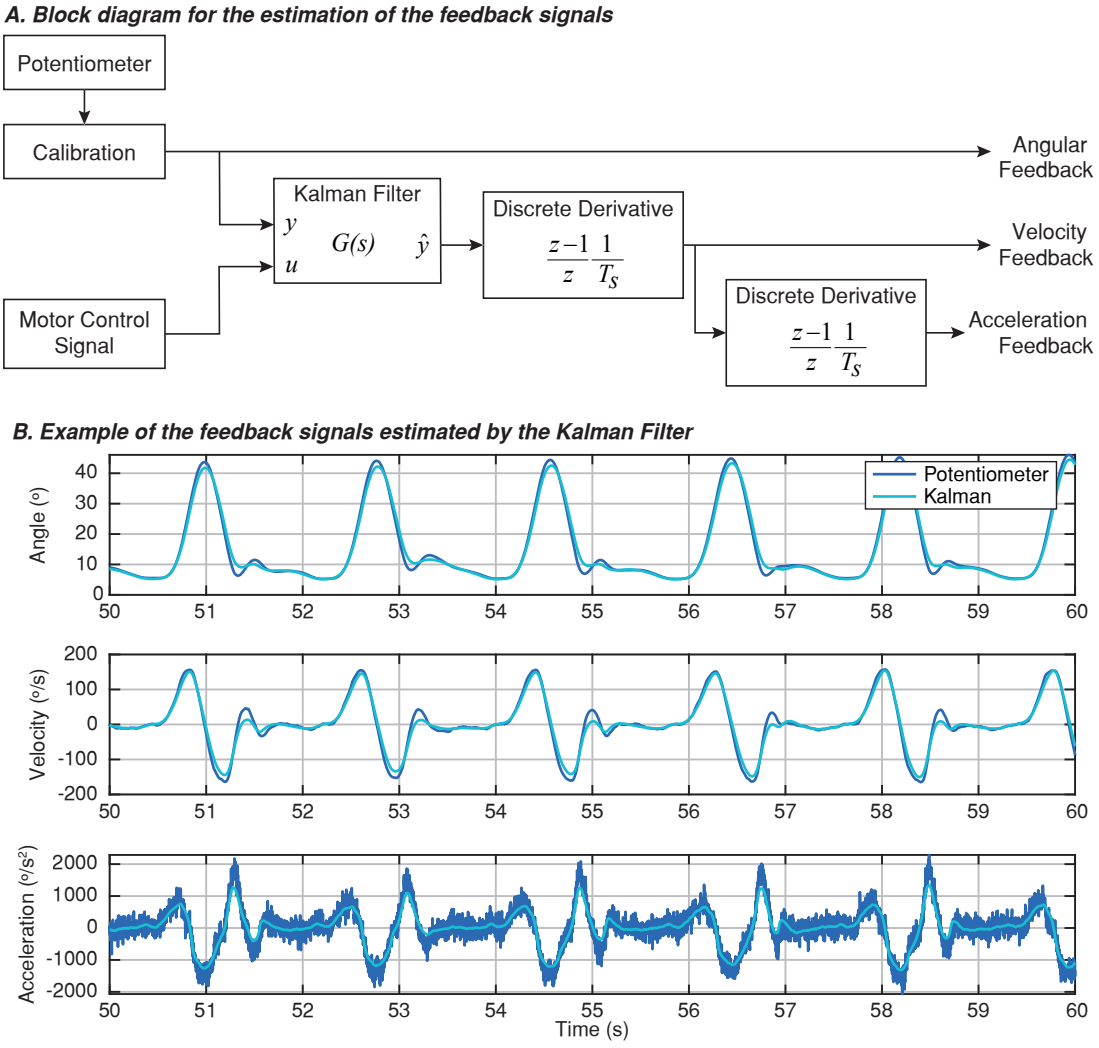

FIGURE 4.6: Potentiometer signal processing using a Kalman filter to calculate the velocity and acceleration feedback. Panel A shows the block diagram for the estimation of the feedback signals. The Kalman filter uses as input the angular feedback (y) and the control signal for the actuator (u) and as the system model ($G(s)$) the identified from REFLEX's experimental data. The estimated angular feedback ($\hat{y}$), which is the output of the Kalman filter, is discretely derived twice to calculate the velocity and acceleration feedback signals. Panel B. compares the original signals obtained by directly deriving the potentiometer measure (in blue) and the resulting signals from the Kalman filter (in cyan).

Experimental trials were also carried out to assess the performance of different impedance models (see figure 4.8). Five different impedance levels were tested during the swing phase of the gait cycle: from the highest level, near to a pure position controller, to a low impedance controller that allows higher motion freedom. A lower impedance level means a lower interaction torque for the same kinematic error, which leads to reduced assistive actions.

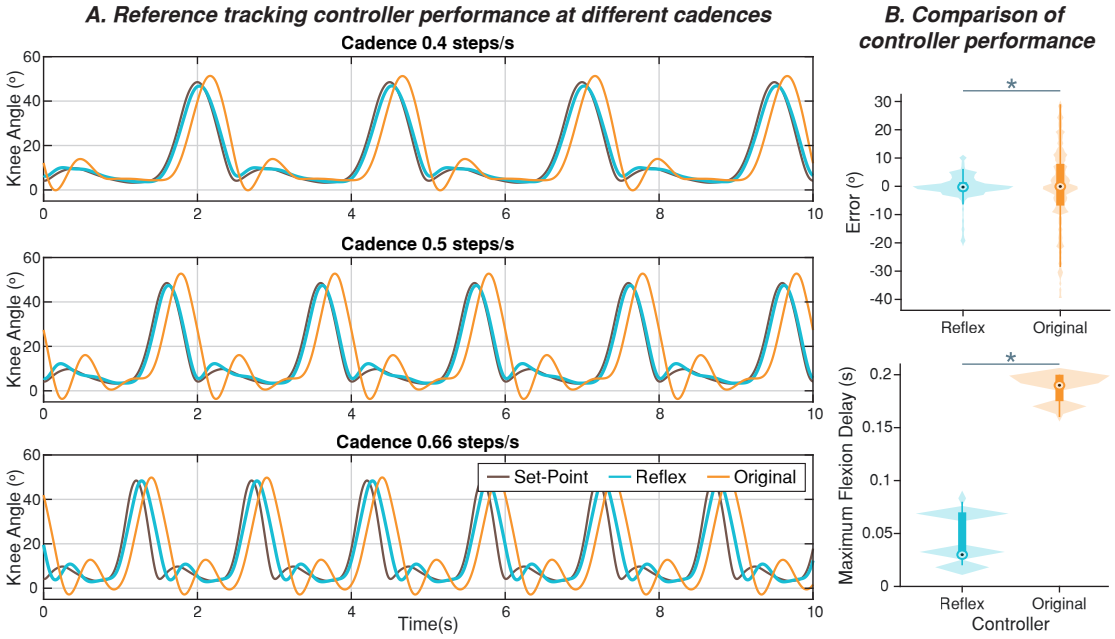

FIGURE 4.7: Results of reference tracking with a high impedance model. Panel A shows results obtained by the REFLEX controller and the former version proposed in [28]. The same angular reference (in brown) feeds both controllers (REFLEX's in cyan and original in orange). Each panel represents data for different gait cadences. Panel B compares tracking errors and delays for both controllers. Violin plots represent the data distribution: areas represent the histograms, while boxplots represent the median and interquartile range. Markers (*) point out significant differences between distributions.

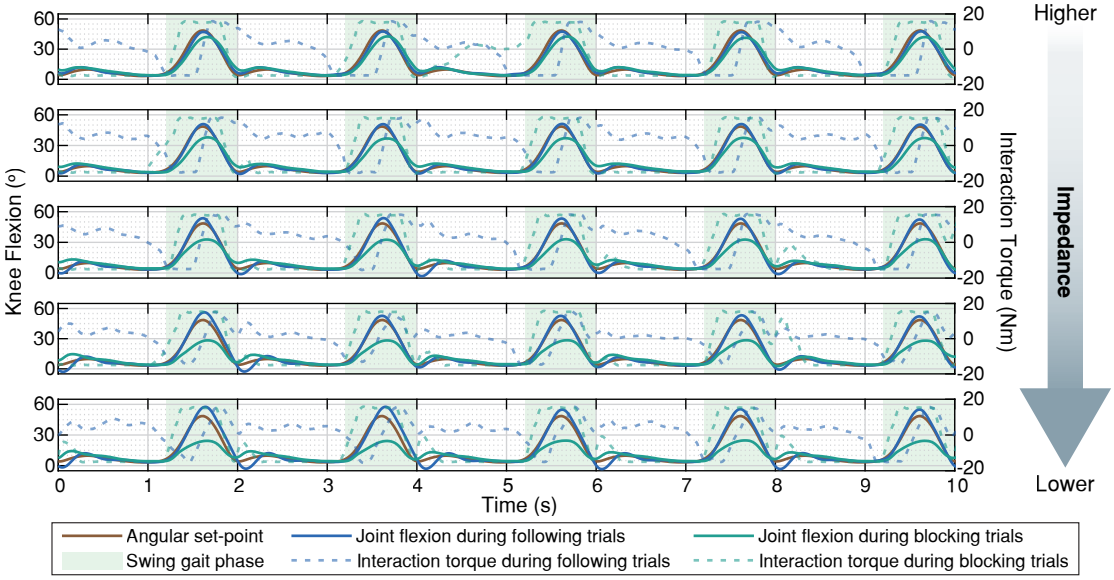

FIGURE 4.8: Effect of different impedance models in REFLEX's control. Each panel shows the joint motion and set-point (in brown) using different impedance models. During the stance phase, the highest impedance model reinforces the joint, not allowing deviations from the reference; conversely, during the swing phase (green areas), different impedance levels implied different assistance. Impedance level during swing decreases from top to bottom panels. Results from two trials are shown: during *following trials* (indigo lines), an interaction torque tried to increase its range of motion; conversely, during *blocking trials* (teal lines), an interaction torque tried to decrease its range of motion. Measured interaction torques are also represented using dashed lines with respect to the right axes.

TABLE 4.1: Results from the comparison between REFLEX and original controllers

Controllers	***Tracking error (º)***	***Time Delay (s)***
REFLEX Controller	-0.4232±4.6193 (4.6382)	0.0448±0.0228 (0.0501)
Original Controller	-0.5471±14.1273 (14.1367)	0.1887±0.0128 (0.1891)

Mean ± STD (RMS value between brackets)

Two trials were used to evaluate the impedance model performance. During them, the action of an external torque was varied: during *following trials* the external torque actively followed the joint's movement to increase its range of motion; conversely, during *blocking trials* the external torque actively tried to block the movement and reduce its amplitude. As shown in figure 4.8, the device's assistance is correctly managed by the impedance controller, increasing the motion freedom by reducing the impedance level. Regardless of the trial, during the stance phase of the gait cycle, the highest impedance model was used, and therefore, low deviations from the angular reference were allowed.

4.4 Experimental validation with human subjects

Once the device was technically verified and found to work properly, the REFLEX prototype was used with human subjects to validate its assistive action. This validation was implemented in two phases. During the first one, the device was tested with healthy subjects to ensure its proper operation during human interaction. Afterward, the prototype was evaluated with stroke patients to assess their reaction to REFLEX assistance.

In total, six voluntary subjects participated in the experiments. Three healthy subjects (3 males, age: 24.7±3.8 years, height: 1.78±0.02 m, weight: 77.7±2.5 kg; mean ± STD) and

TABLE 4.2: Stroke subjects' demographic data

Id Subject	***P1***	***P2***	***P3***	**Average**[a]
Age (years)	63	57	54	58±4.6
Heigth (m)	1.8	1.7	1.7	1.74±0.05
Weigth (kg)	83	84	60	75.6±13.6
Time after stroke (months)	11	7	9	9±2
Sex	Male	Male	Male	
Hemiparetic side	Left	Right	Left	
Stroke	Cortical ischemic	Subcortical hemorrhagic	Cortical ischemic	

[a]Mean±STD

three chronic stroke patients (demographic data summarized in table 4.2) were recruited for this experiment. All subjects gave their informed consent for the experiment; the study was conducted in accordance with the Declaration of Helsinki, and it was approved by the local ethics committee. All subjects were instructed to walk on a treadmill at a constant gait speed during 5 minutes trials. All subjects carried out four different kinds of trials: (1) *NoExo*: subjects only wore the inertial sensors and the insole pressure sensors to acquire their basal motion; (2) *Free*: subjects wore the exoskeleton although the actuator was mechanically decoupled, so it enabled the free movement of the knee; (3) *Echo*: the device provided gait assistance following the Echo-control strategy (see section 3.3.1); and (4) *Pattern*: the device provided gait assistance following the Adaptive Healthy Pattern strategy (see section 3.3.2). During these trials, all subjects used the tethered version of REFLEX, and stroke patients wore a safety harness that did not support any weight. Prior to the execution of the trials, the gait velocity was self-selected to a comfortable level by the subjects.

The subjects rested between trials for at least five minutes to avoid adaptation and learning effects from trial to trial. In addition, only the two last minutes of the trials were processed to evaluate the gait once the steady-state was reached. For the data processing, the beginning of each step was considered when the insole pressure sensors detected the heel strikes. All experimental data were recorded at 50 Hz.

4.4.1 Validation on healthy subjects

The following results are from the experiments conducted to understand how the assistance provided by the exoskeleton affects the gait of healthy subjects. Figure 4.9 illustrates, as an example, the knee phase portraits during one experimental trial with one healthy subject. Comparing how the phase portraits evolved across trials enables to visualize how the movement of both knees (actuated and not) changed according to the REFLEX operation mode. Panel A in figure 4.10 shows the average phase portraits of both legs during trials and how the similarity measured in the *NoExo* trial decreased due to wearing the robot in the *Free* trial. However, the robot's action actively improved similarity during the *Echo* and *Pattern* trials.

To evaluate the similarity between phase portraits, the similarity metric previously defined in equation 3.19 was used. Panel B of figure 4.10 shows the results of comparing different median phase portraits according to this metric. Panel B1 compares assisted and master motion in each experimental trial. The results indicate that the same behavior was replicated in all subjects. Wearing the device hampered the similarity between limbs, i.e., the symmetry; however, the provided assistance partially compensated for the effect of wearing the device since the similarity increased with respect to the *Free* condition. Nonetheless, it did not reach the similarity level of the *NoExo* trials. Only the *Pattern*

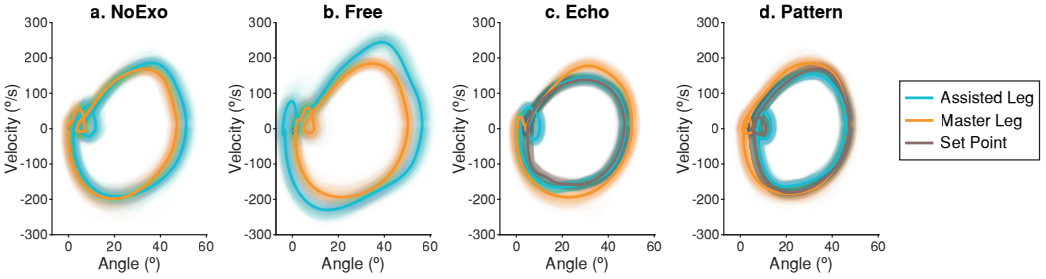

FIGURE 4.9: Knee movement's phase portrait from the trials performed by a healthy subject (HS1). Cyan lines correspond to the assisted knee's movement while orange lines correspond to the master knee's movement; brown lines correspond to the set point followed by the robot. Solid lines represent the median movement and semi-transparent lines show individual steps. When the user wears the robot, the assisted leg's phase portrait changes in hip and knee joints; however, the action of the robot during *Echo* and *Pattern* conditions compensates for the effect of wearing the robot and makes the assisted leg's phase portrait closer to the master leg's portrait.

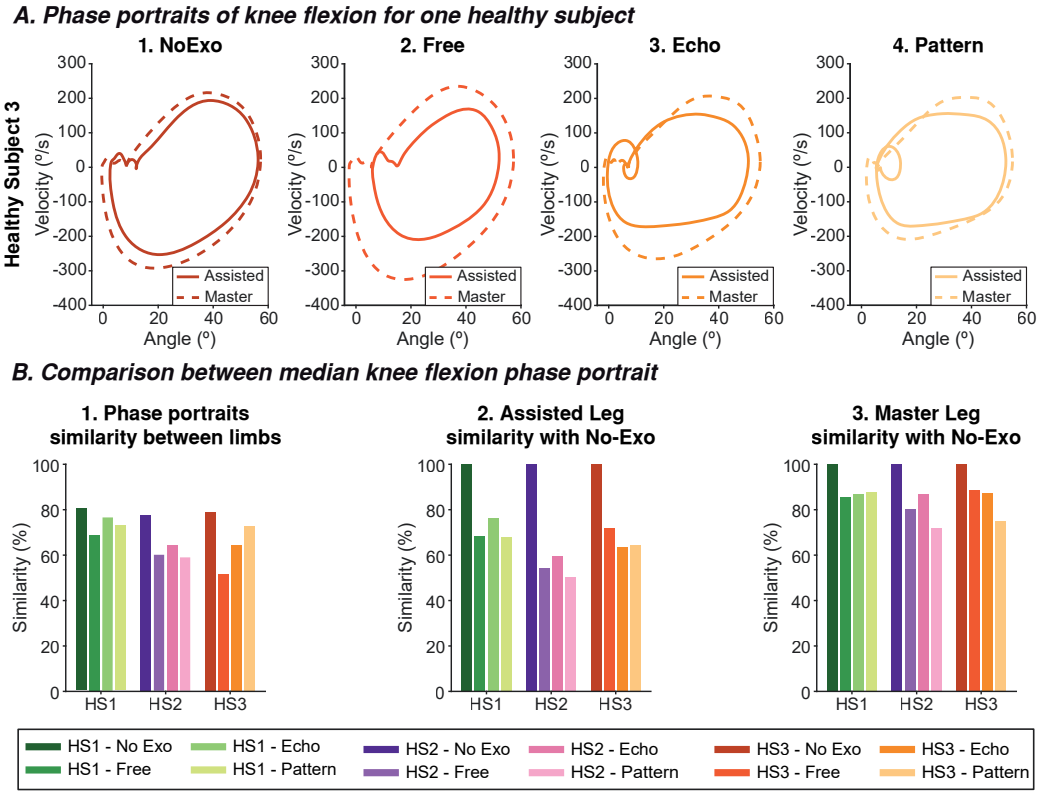

FIGURE 4.10: Comparison between master and assisted knee phase portraits across trials when REFLEX prototype provides different kinds of assistance to healthy subjects. Panel A. shows the median phase portrait for each leg; columns 1-4 include information for each experimental condition. Solid lines represent the assisted leg, and dashed lines represent the master leg. Panels B. show the similarity between the areas of the phase portrait: Panel B1 represents the similarity between both limbs under each experimental condition, and panels B2 and B3 represent the similarity between the movement of the current experimental condition and the movement during *NoExo* for each leg. Across the figure, data for the same patient is represented in the same color (green for HS1, purple for HS2, orange for HS3) while the brightness indicates the experimental condition (from darkest to lightest: *NoExo*, *Free*, *Echo*, and *Pattern*). Similarity decreases because of wearing the robot; however, the assistance provided by the exoskeleton actively improves similarity in all patients.

strategy in Subject 2 did not improve the similarity with respect to the Free condition. Changes in inter-limb similarity were found to be due to variations in the assisted leg (figure 4.10, panel B2), but also due to adaptations in the master leg's motion (figure 4.10, panel B3).

To evaluate the performance of the assistance, the effect of the exoskeleton's action over the range of motion (RoM) of the knee and the gait cycle percentage of the maximum knee flexion was also assessed (figure 4.11). The metric value in each step was considered to create a distribution for each subject during each experimental condition. After checking the non-normality of the data (Kolmogorov-Smirnov test; $P < 0.005$) and the heteroscedasticity (Levene test; $P < 0.005$), significant differences between experimental conditions were looked for (Kruskal-Wallis test; $P < 0.005$).

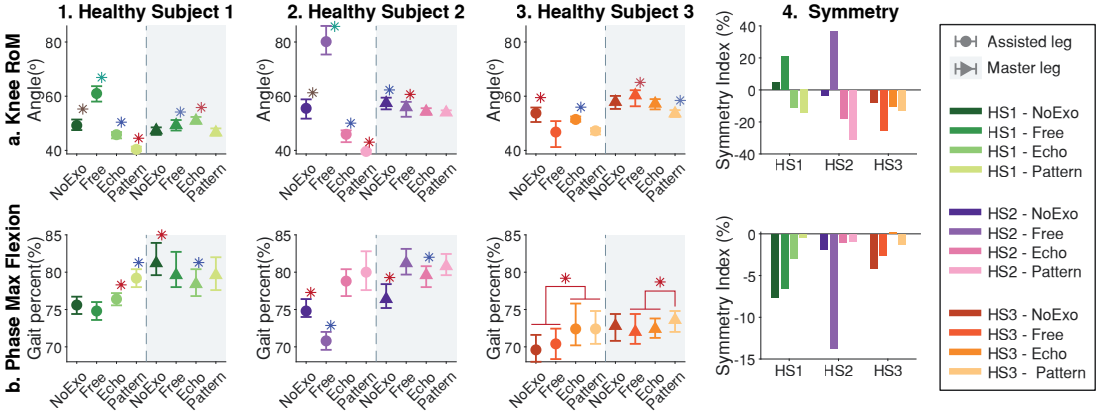

FIGURE 4.11: Knee kinematics symmetry for healthy subjects. Rows a and b represent the knee Range of Motion and the phase at maximum flexion for the knee. Columns 1-3 represent the result for each subject; markers indicate the median value and whiskers the 10-90 percentiles. Column 4 represents the symmetry index for each subject under each experimental condition; notice that symmetry indexes closer to 0 mean a higher symmetry between limbs. Across the figure, colors represent the same healthy subject (HS1 in green, HS2 in purple, and HS3 in orange), and the brightness represents the experimental condition (from the darkest to the lightest: *NoExo*, *Free*, *Echo* and *Pattern* correspondingly) and the shape of the marker represents the assessed limb (circle for the assisted limb and triangle for the master leg). Markers (*) show significant differences between experimental conditions within a subject's limb.

The symmetry was evaluated using the Symmetry Index (SI) introduced by Arazpour et al. [12]:

$$SI\,(\%) = \frac{\bar{X}_A - \bar{X}_S}{\frac{1}{2}\left(\bar{X}_A + \bar{X}_S\right)} \times 100 \tag{4.3}$$

where $\bar{X}_A$ and $\bar{X}_S$ are the mean value for a metric in the assisted and sound (or master) leg, respectively. A SI of zero value means a complete symmetry, so a higher SI means a higher asymmetry in the metric. The fourth column of figure 4.11 shows that the RoM and the phase of maximum knee flexion are more symmetric during assisted trials than during the *Free* trials. However, although the highest symmetry for the phase of

maximum knee flexion was achieved during assisted trials, the highest RoM symmetry is yielded during the *NoExo* trial.

4.4.2 Validation on hemiparetic stroke patients

During this second validation phase, the prototype's performance with real hemiparetic patients was evaluated. To this end, the main interest was to assess how the patients reacted to the assistance provided by the prototype; an example of the data recorded for a patient is represented in figure 4.12. To compare the motion dynamics in both knees, the median phase portraits of the flexion/extension movement were used (figure 4.13, panel A). Their similarity was assessed by using the equation 3.19; results are represented in panel B of figure 4.13.

As shown in panel B1 of figure 4.13, the robot assistance always improved the similarity between the motion of both limbs with respect to the motion in the *Free* condition. In two out of three patients (P1 and P3), wearing the robot (*Free* condition) hampered the

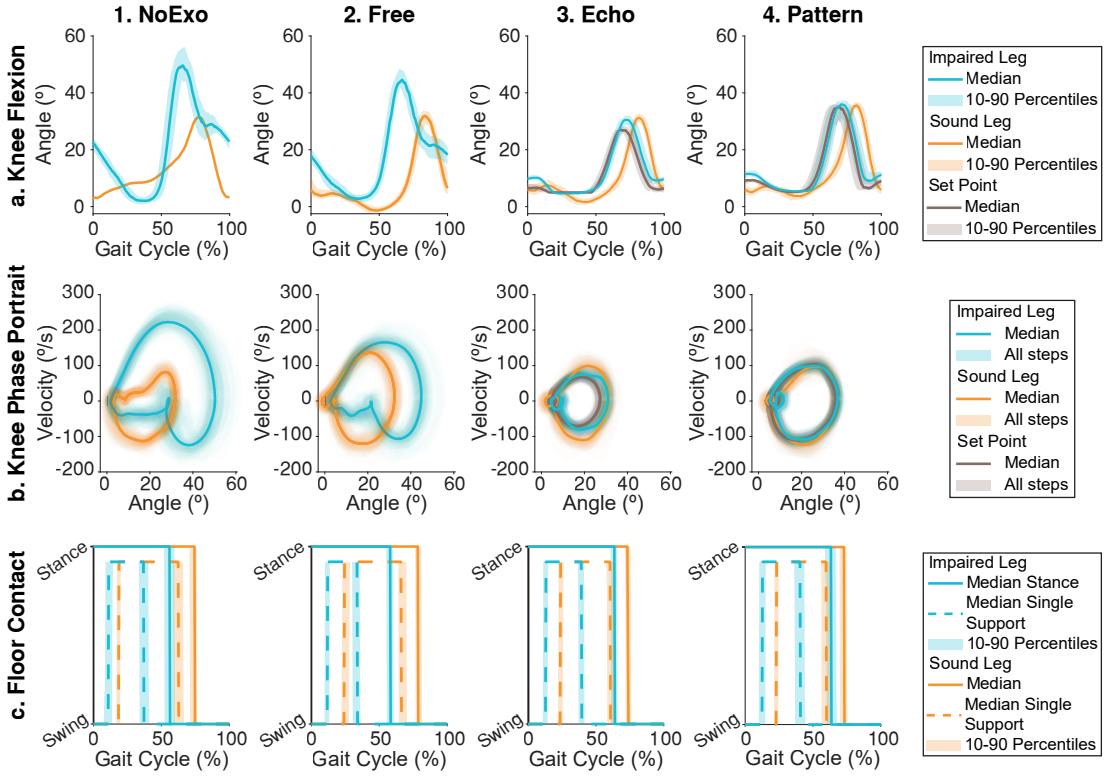

FIGURE 4.12: Example of step data from a hemiparetic patient (P2) during the different experimental conditions. Columns 1-4 include information for each experimental condition: *NoExo*, *Free*, *Echo*, and *Pattern* respectively, while rows a-c show the knee kinematics (a), its phase portrait (b), and the foot contact with the floor (c). Information is represented for both legs: the paretic leg is in cyan while the sound leg is in orange. The exoskeleton set point is also represented in brown for the assistive experimental conditions.

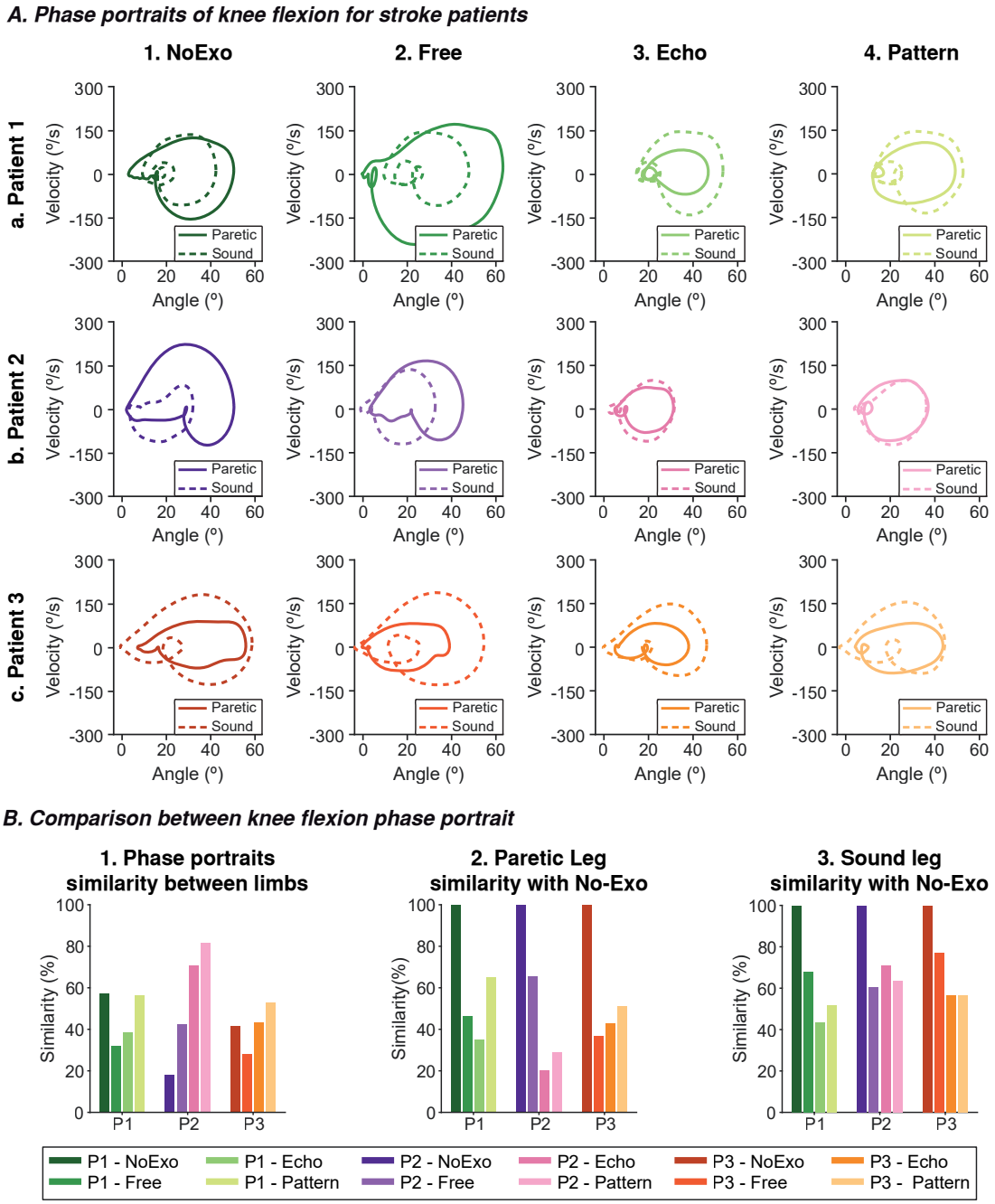

FIGURE 4.13: Knee flexion phase portraits for three stroke patients during assisted and unassisted trials. Panel A shows the median phase portrait for each limb, columns 1-4 include information for each experimental condition, while rows A-C show the data for the three patients. Solid lines are used for the impaired leg, while dashed lines are used for the sound leg. Panel B shows the similarity between phase portraits: panel B1 represents the similarity between both limbs under each experimental condition, and panels B2 and B3 represent the similarity between the movement of the current experimental condition and the movement during *NoExo*. Across the figure, data for the same patient is represented in the same color (green for P1, purple for P2, and orange for P3) while the brightness indicates the experimental condition (from darkest to lightest: *NoExo*, *Free*, *Echo*, and *Pattern*).

symmetry in the motion; however, the action of the robot compensated for this effect (P1 during *Pattern* and P3 during *Echo*) or even increased the symmetry with respect to the NoExo condition (P3 during *Pattern*). In Subject P2, wearing the exoskeleton increased the symmetry, and the exoskeleton's action even enhanced this improvement. In all subjects, the *Pattern* strategy led to a more symmetric motion than the Echo strategy.

Importantly, panels B2 and B3 of figure 4.13 show the limb motion similarity with its movement during *NoExo* trials for the assisted and non-assisted legs, respectively. The motion of both legs changed due to the exoskeleton's action, and therefore, the assistance not only acted over the movement of the assisted leg but also affected the movement of the non-assisted leg to attain a more symmetric gait.

To evaluate the performance of the controllers, the symmetry of the RoM and the phase of maximum knee flexion in both legs were evaluated (figure 4.14) by using the symmetry index defined in the equation 4.3 (represented in the fourth column of figure 4.14). The robot's action yielded more symmetric RoMs in all patients than the *Free* condition; in addition, pattern assistance and echo assistance in P1 and P2 attained a higher RoM symmetry even compared with the *NoExo* condition. The effect of the mass of the robot was heterogeneous: patients P1 and P3 worsened the RoM symmetry while P2 improved it. The symmetry of the maximum flexion phase decreased because of wearing the exoskeleton in all patients. However, the robot assistance compensated for this effect and improved the symmetry with respect to *NoExo* in all patients and under all control strategies, except P3 during *Echo* that seemed not to be affected.

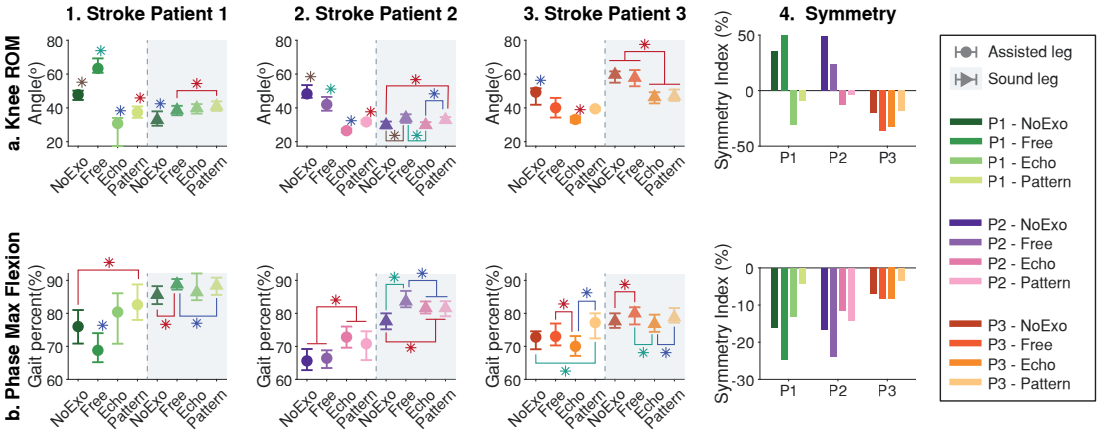

FIGURE 4.14: Knee kinematics symmetry for stroke patients. Rows a and b represent the knee RoM and the phase at maximum knee flexion. Columns 1-3 represent each subject's result (median value and 10-90 percentiles). Column 4 represents the SI for each subject under each experimental condition; notice that symmetry indexes closer to 0 mean a greater symmetry between limbs. Across the figure, the same color represents the same patient, the brightness gradation represents the experimental condition and the shape of the marker represents the assessed limb (see the legend for details). Markers (*) show significant differences between experimental conditions within a subject's limb.

The effect of the assistance on the compensation mechanisms developed by the patients was also assessed. By using the floor contact information and the IMU data, the influence of the exoskeleton on gait parameters related to compensatory strategies was analyzed, concretely: (a) step length, (b) step time, (c) step velocity, (d) single-support duration, (e) stance phase duration, and (f) swing time (rows A-F of figure 4.15).

The symmetry index was used to evaluate the robot's action with respect to these metrics (fourth column of figure 4.15). Overall, the assistance provided by the robot led to more symmetric features compared with the *NoExo* trials or at least compensated for the detrimental effect of wearing the extra mass of the device. However, patients presented a heterogeneous response for some features.

Step length symmetry was improved during all assistive trials compared with the basal condition (excepting *Echo* in P3). However, each patient responded differently: improvements in P1 were because of wearing the robot (assistive strategies and *Free* condition yielded the same results), P3 improvements were also because of wearing the device, although the assistance decreased this symmetry (nonetheless, the *Pattern* condition supposed higher symmetry than the *NoExo* condition), and P2 reported symmetry improvements even when wearing the device resulted in its decrease (panel 4A of figure 4.15).

For all patients, wearing the robot caused a decrease in the step time symmetry (panel 4B of figure 4.15). However, this effect was compensated by the action of the assistive strategies, and P2 even increased step time symmetry with respect to his basal condition. Regarding the step velocity (panel 4C of figure 4.15), both assistive strategies led to an increase of symmetry in P1 and P2 compared with the *NoExo* condition, although this was partially attained during the *Free* trial in P1; for P3, the *Pattern* assistance yielded the same symmetry improvement as the *Free* condition with respect to the *NoExo* trial, although the *Echo* assistance supposed a decrease in the step velocity symmetry.

These improvements in step velocity symmetry occurred because all patients increased the step velocity of the assisted leg and reduced it in the non-assisted leg (P1 and P2) or increased it at a lower level (P3). The origin of these velocity changes was heterogeneous across patients, and the changes are related to the patient's own strategies to cope with the robot's actions. For instance, P1 increased the step length and reduced the step time in the paretic leg while reducing the step length of the sound leg. P2 increased the step length and time in the paretic leg while maintaining step length and increasing the step time in the nonparetic leg. Finally, symmetry improvement in P3 was due to increasing step length and reducing step time in the paretic leg, and increasing the step length of the nonparetic leg.

Regarding symmetry of the stance and swing phases of the gait, the assistance provided by the exoskeleton always led to a more symmetric single-support and stance step

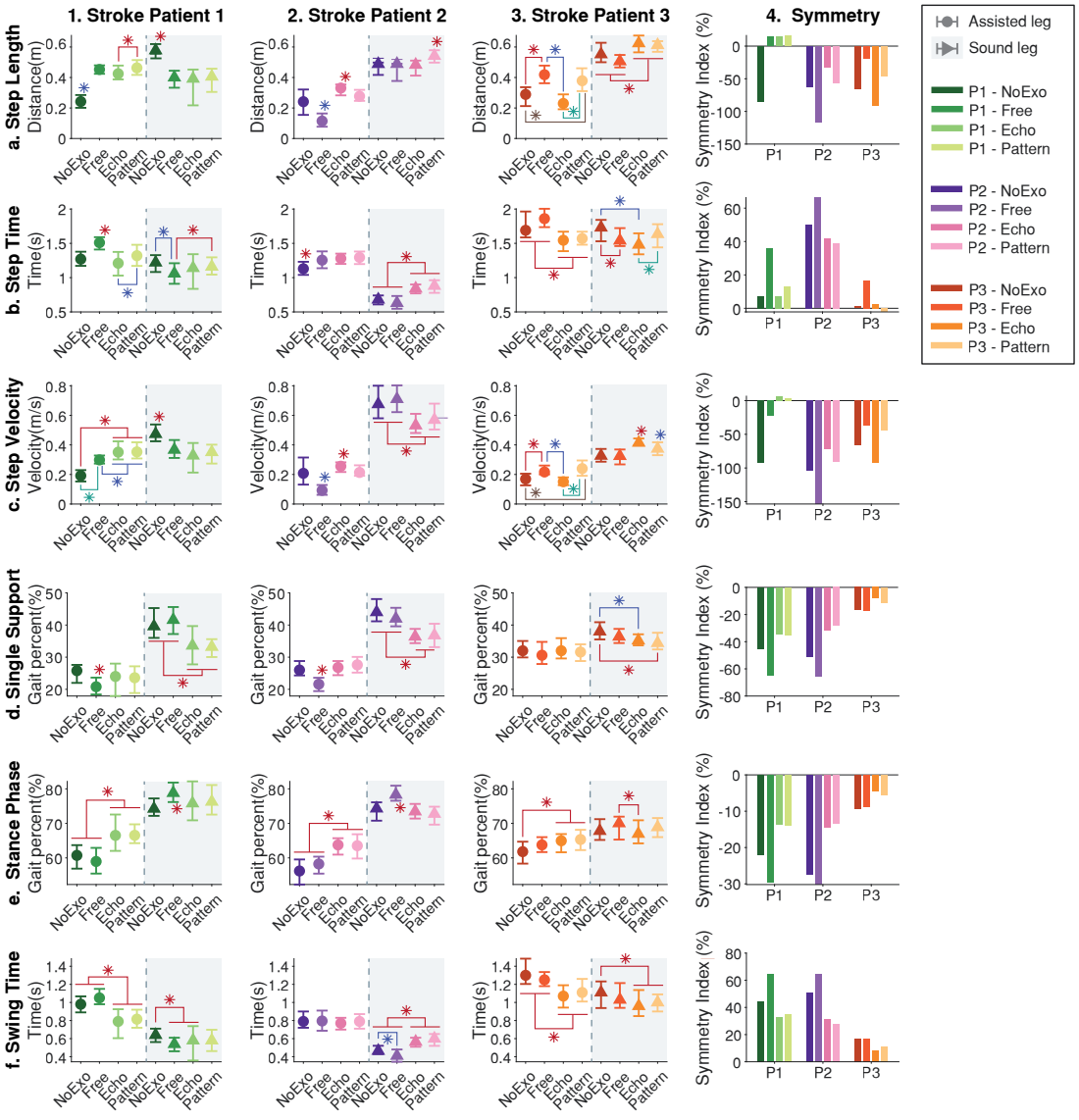

FIGURE 4.15: Gait features symmetry for stroke patients. Rows a to f include different gait metrics: step length (a), step time (b), step velocity (c), single-support duration (d), stance phase duration (e), and swing time (f). Columns 1-3 represent the result for each subject; markers indicate the median value and whiskers the 10-90 percentiles. Column 4 represents the symmetry index for each subject under each experimental condition; notice that those symmetry indexes closer to 0 mean a higher symmetry between limbs. Across the figure, colors represent the same patient (P1 in green, P2 in purple, and P3 in orange), and the brightness represents the experimental condition (from lightest to darkest: *NoExo*, *Free*, *Echo* and *Pattern* correspondingly) and the shape of the marker represents the assessed limb (circle for the assisted limb and triangle for the sound leg). Markers (*) show significant differences between experimental conditions within a subject's limb.

percentages compared to the *NoExo* condition (panels 4D-4E of figure 4.15); even when wearing the robot resulted in less symmetry than the basal condition (P1 and P2). Equally, the assistance provided by the robot improved the symmetry of swing time in all patients compared to *NoExo*, even when Free trials exhibited a decrease of symmetry in this metric (panel 4F of figure 4.15).

All patients attained symmetry improvements in the single-support and stance phases by increasing their duration for the assisted leg and/or reducing these durations for the unassisted leg. Conversely, the strategy followed to improve symmetry in the swing time differed between subjects: P1 and P3 reduced swing time for both legs while P2 only increased it for the non-assisted leg.

4.5 Discussion on gait adaptation to assistance

This chapter introduces the proof of concept of the REFLEX exoskeleton, which is aimed to serve as a tool to investigate the effects of unilateral assistance in hemiparetic gait. Experimental tests have been carried out to evaluate the effects of the two proposed controllers providing gait assistance based on the motion of the sound leg of hemiparetic patients, looking for natural coordination between assisted and unassisted joints.

The results indicated that healthy subjects decreased the similarity between the motions of both legs because of wearing the exoskeleton's extra load. Although robot assistance partially counteracted this effect, the device could not achieve the symmetry that these subjects showed during normal walking. Interestingly, the symmetry improvements yielded by the exoskeleton action were not only due to changes in the assisted leg; rather, the non-assisted leg's motion also evolved to attain a higher level of symmetry. Therefore, it can be concluded that the healthy subjects reacted to the assistance provided by the robot by actively changing their gait pattern to attain a more symmetric gait. This may be justified by the influence of the proprioceptive changes produced by the exoskeleton action on the gait pattern generators [137, 321].

The effect of the assistance on hemiparetic gait was homogeneous. All subjects increased the similarity between the motion of both limbs due to the provided assistance compared with the *Free* condition. However, despite these improvements, the response with respect to the basal condition differed between subjects. Three out of six experimental conditions improved the symmetry with respect to the basal condition, two out of six compensated for the hampering effect of wearing the robot, and only one out of six could not fully compensate for it.

Notably, the *Pattern* strategy achieved better results than the *Echo* strategy in assisting post-stroke hemiparetic subjects. Under the *Pattern* strategy, two out of three patients

improved the motion symmetry with respect to their basal conditions, and only one subject compensated for the effect of wearing the robot. Conversely, under the *Echo* strategy, only one subject improved with respect to his basal condition, one subject compensated for the effect of wearing the device, and one subject could not compensate for this effect.

The worse performance of the *Echo* strategy in hemiparetic patients is due to the low repetitiveness in the movements of their lower limbs [168] compared with healthy subjects. As *Echo* strategy relies on the repetitiveness of joints' motion (see section 3.3.1), this lack of similarity in the sound limb movement negatively affects the performance of this strategy compared with *Pattern* (see figure 4.16).

Compared with the *Free* condition, the assistance results were similar for both kinds of subjects (healthy and hemiparetic), as the assistance increased the similarity of the motion, the RoM, and the phase of maximum flexion of the knee joint. However, they differed in comparing the results with their basal condition. While the robot was unable to improve the gait symmetry in healthy subjects, it was able to assist the gait of hemiparetic subjects in improving symmetry.

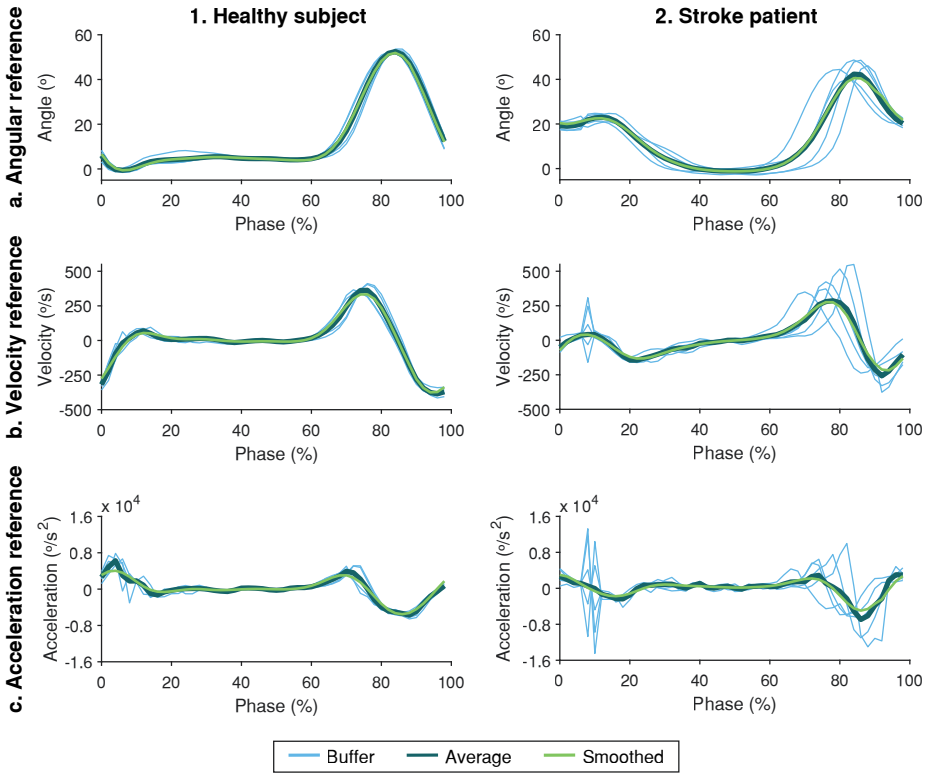

FIGURE 4.16: Example of the three references generated by the Echo strategy (angle, velocity, and acceleration for rows a-c) during trials with a healthy subject (column 1) or a stroke patient (column 2). Light blue lines represent the content of the five-step buffer, the dark cyan line is the average step, and the green line is the smoothed average step that serves as the pattern reference.

The assistance provided by the robot also led to more symmetric gait features in stroke patients. The *Pattern* strategy improved the step length, time, and velocity symmetry in all patients with respect to their basal condition, or, at least, it compensated for the hampering effect of wearing the robot. However, the *Echo* strategy could not achieve these improvements in one out of the three hemiparetic patients. Similarly, robotic assistance led to more symmetric single supports, stance phases and swing times. In these cases, both assistive strategies achieved similar results.

These results indicate that the device's action can assist the gait in hemiparetic patients in such a way that classic compensations to attain a functional gait are decreased. In this sense, the robot's action increased the stance phase in the paretic leg and reduced the single-support phase in the nonparetic leg, compensating for typical disturbances in hemiparetic gait [21]. The assistance provided by the exoskeleton also yielded a more symmetric step length, time, and velocity. These improvements could be associated with decreased asymmetric limb loading and gait inefficiency [275] and can improve patients' balance during walking [203].

Notably, these symmetry improvements are not only due to changes in the assisted limb. In contrast, the motion of the non-assisted leg of the patients also evolves to attain a more symmetric gait globally. Patients seemed to integrate feedback from the assisted leg to adjust the action of the non-assisted limb, improving gait performance and stability [336]. This may be explained by the action of central pattern generators located in the spinal cord using the feedback from proprioceptive muscular and tendinous receptors that inform the nervous system of applied loads and forces due to the exoskeleton action [321].

This assistance integration could release the nonparetic leg from excessive loading patterns that may lead to secondary musculoskeletal complications [232], since temporal asymmetry correlates with increased vertical ground reaction forces in the nonparetic leg [175]. Interestingly, these adaptations in the non-assisted leg were attained in a short time (5 minutes) and occurred naturally without following any kind of instruction. Adaptations in the non-assisted leg were also reported by Chinimilli et al. [61], although they involved healthy subjects in their trials. They found that unilateral knee assistance increased the unassisted leg's stability due to interlimb coordination in this population. For stroke patients, adaptations in the non-assisted leg were also reported during early robotic rehabilitation with the single-leg version of the HAL exoskeleton [289].

These results on gait symmetry improvements are similar to those previously reported by other authors who aimed to assist impaired gait unilaterally. For example, Arazpour et al. described an active KAFO to improve symmetry in poliomyelitis subjects based on an FSM controller and reported symmetry improvements in swing time, stance phase percentage, and knee flexion during swing [12]. Similarly, Beyl et al. reported timing symmetry improvements in one multiple sclerosis patient when assisted by the KNEXO

prototype [37]. The unilateral exoskeleton robot developed by Shenzhen University [380] reported improvements in the range of motion of the joints of three hemiparetic subjects. However, their controller was based on detecting the heel-strike event to trigger the assistive action. Kawamoto et al. described a control strategy based on the kinematic of the non-paretic leg, similar to the proposed *Echo* control, that reported significant symmetry improvements in one stroke patient while HAL exoskeleton assisted his gait [174]. However, in contrast with the presented approach, the control paradigm of these examples was based on the detection of gait events, and therefore, they were not adaptive in real-time to changes in gait frequency.

In contrast, the ALEX III prototype used a pool of AOs and nonlinear filters to reconstruct the joint patterns of the nonparetic leg that acted as references for the hip and knee of the paretic limb [399]. They tested this approach in three healthy subjects simulating impairments in one leg by wearing a load on the ankle and reported gait symmetry improvements due to the action of the device. Although they reported symmetry improvements, with the presented approach, the origin of these improvements was found to be twofold: the assistance of the paretic leg and the adaptation of the non-assisted leg.

In contrast to previous studies, the results of assisting the paretic leg with the kinematics of the nonparetic leg or with a standard healthy pattern were compared. Considering the global results with stroke patients, the *Pattern* strategy seemed to perform better than the *Echo* strategy. This suggests that providing assistance according to a normalized healthy pattern would lead to better outcomes than assisting with the motion of the nonparetic leg of the subject. As changes were obtained in the motion of both limbs, assisting the paretic limb with a healthy motion could lead to the nonparetic leg also evolving to a healthier pattern without compensation mechanisms. Hypothetically, this approach might improve gait beyond compensatory strategies arising from hemiparesis, promoting new functional patterns with lower energetic costs.

4.6 Conclusions

This chapter presented the REFLEX prototype, an active KAFO that assists the knee flexion/extension of the impaired leg of stroke survivors. This device reinforces the paretic joint during the stance phase of the gait and guides its movement during the swing according to the motion of the sound limb to ensure proper and natural inter-joint coordination.

Experimental results with three healthy subjects and three stroke survivors revealed that the REFLEX prototype is able to assist the gait of hemiparetic subjects coordinately with the movement of the non-paretic leg. The patients showed improved spatial

and temporal symmetry due to the assistance provided by the exoskeleton. These improvements were related not only to the robotic exoskeleton's motion guidance but also to the adaptation that occurred in the non-assisted limbs, which seemed to decrease their compensatory strategies.

Chapter 5

EVALUATION OF REFLEX ASSISTANCE INTEGRATION IN STROKE PATIENTS

Preliminary results about how hemiparetic patients reacted to REFLEX's assistance were quite promising. They seemed to indicate that the robotic assistance was properly integrated by stroke survivors, who were able to adapt the motion of the non-assisted limb and, therefore, reduce their compensation mechanisms.

This chapter presents the second experimental validation carried out to deepen into the effects of REFLEX's assistance in hemiparetic subjects. During this study, special attention was paid to the effect produced in the muscular activity as it would be a metric to evaluate the embodiment of this technology. Significant differences were obtained at the subject level due to the assistance; however, the high dispersion of the measured outcomes avoided extracting global effects at the group level.

5.1 Introduction

The results obtained during the preliminary validation of REFLEX were promising and suggested the proper integration of the assistance in a small cohort of stroke patients. The *Pattern* strategy was especially interesting, as it led to better results and a more reliable robot performance than the *Echo* strategy (see the previous chapter for details). However, some aspects of this gait adaptation still remain elusive.

The main hypothesis of this dissertation is that if REFLEX's action is properly embodied, it will lead to adaptations and gait changes. These changes can be kinematic adaptations, as preliminary results seemed to indicate. However, if the robot's action is

integrated by the nervous system, the observed changes should imply modifications in muscle recruitment [240].

Recently, authors described muscular adaptations due to robotic assistance. Gordon et al. reported that unimpaired subjects could reduce soleus activity while assisted by an ankle exoskeleton [125]. Similarly, the ankle exoskeleton used by Steele et al. also reduced healthy ankle plantarflexor activity due to its assistance during gait [340]. Wehbi et al. used a knee exoskeleton to assist healthy knee flexion during swing, reducing the muscular effort of the short head of the biceps femoris and the vastus medialis [379]. Lee et al. also reduced healthy knee extensor activity using a robotic knee exoskeleton, although they assisted the stance phase of the gait and validated the system during inclined and declined walking [195]. Instead of a rigid robot, Sridar et al. used a soft knee exoskeleton to assist knee extension during gait, reducing quadriceps activity in healthy subjects [337, 338].

Acosta-Sojo et al. also evaluated the muscular response of healthy subjects to the assistance provided by an ankle exoskeleton during walking [2]. A variable percentage of participants reduced medial gastrocnemius and tibialis anterior activity (60% and 80% respectively) due to the robot assistance, and they pointed out that this reduction may affect the antagonist muscular effort as a result. However, muscular responses highly varied between individuals, hampering the identification of global effects in this sense. Due to this discrepancy, their study concluded the necessity of understanding these individual adaptations to tailor the exoskeleton performance.

The above-mentioned papers recruited unimpaired walking subjects to validate the presented devices. Their results demonstrated that healthy subjects are able to integrate the robotic assistance to reduce muscular activity and, therefore, the energetic cost of walking, increasing their endurance. However, authors usually do not analyze the assistance integration when impaired subjects are involved in the experiment since the primary purpose of this assistance is to achieve an autonomous and stable gait (see section 1.4.6 for details). This shows a lack of understanding of how impaired walking subjects react to robot assistance, especially whether they were able to integrate the robot action and consequently adapt their muscular activity to it.

The aim of this chapter is to further understand the effects of REFLEX assistance in hemiparetic patients, focusing not only on the kinematic adaptations but also on the muscular response that would indicate the proper integration of the robotic action. Firstly, this chapter describes the experimental protocol developed to evaluate these effects, then the metrics and the conducted data analyses are presented. The obtained results are reported and analyzed individually per subject and globally to detect significant group effects. The obtained conclusions are discussed at the end of this chapter.

5.2 Experimental procedure

Post-stroke hemiparetic subjects were recruited for the experiment. They wore the REFLEX prototype in the paretic leg while walking on a treadmill. Additionally, as a security measurement, they also wore a security harness that did not support any of the patient's weight. Figure 5.1 shows one of the patients during the experimental sessions.

FIGURE 5.1: A patient during the experimental validation. He was wearing the REFLEX prototype while walking on the treadmill. He was also wearing a security harness that did not support the patient's weight.

This protocol aimed at assessing the reaction of the patients to the assistance provided, specifically, the effects on their gait and the possible integration of this assistance by the nervous system that should be reflected by changes in muscular activity. Additionally, this protocol also aimed to assess patients' reactions to variations in gait speed.

Apart from the exoskeleton and the inertial sensors used in the preliminary validation, this experimental set-up included wireless EMG sensors (Trigno Avanti sensors from Delsys Inc, USA) to record muscular activity from representative lower limb muscles of both legs: rectus femoris, biceps femoris (long head), tibialis anterior and medial gastrocnemius. The *Seniam* guidelines [138] were followed to ensure the proper quality of the EMG recordings. In this regard, the muscles' bellies were identified to place the electrodes after shaving and cleaning the zone with alcohol. Figure 5.2 shows the referred sensor set-up.

The proposed experimental protocol was composed of one training session and two measurement sessions separated by one or two days each, as illustrated in figure 5.3,

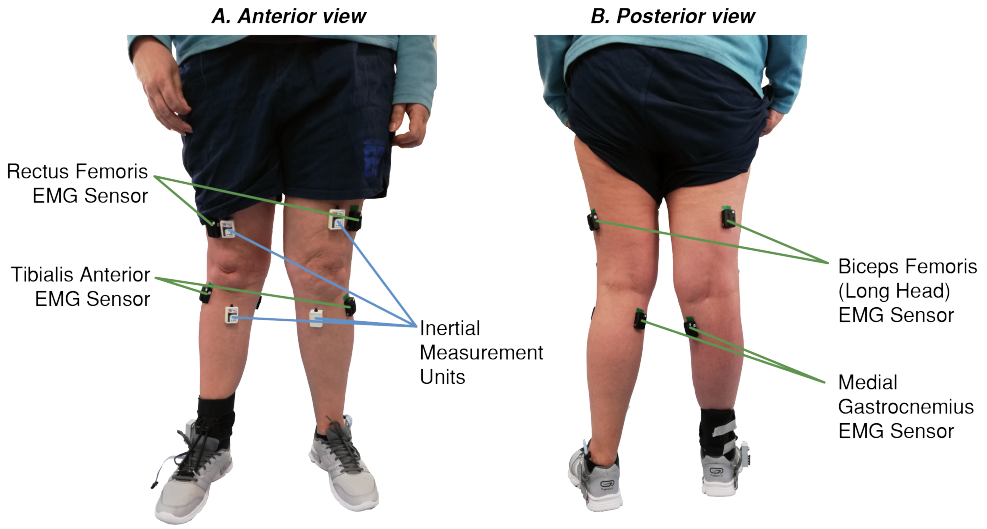

FIGURE 5.2: Anterior (panel A) and posterior (panel B) view of the sensors set-up during the experimental validation. EMG sensors were placed in the Rectus Femoris, Tibialis Anterior, Biceps Femoris (long head), and Medial Gastrocnemius. Inertial sensors were placed in both thighs and shanks of the subject.

panel A. The objective of the training session is twofold: to establish the comfortable and maximum gait speed of the patient while walking with and without the robot, and to enable patients to get used to it. During this session, patients walked with the device for approximately thirty minutes, with three resting periods of five minutes.

Also during this first session, several clinical tests were carried out to measure the physical and cognitive state of the patients and their walking ability. Besides, a sensory examination was carried out as a security procedure to evaluate the subjects' perception and ability to detect forces, pressure, and light touch. The purpose of this procedure was to ensure whether we could rely on the patients' perception to avoid excessive pressure that could be harmful. All patients showed limited perception in their paretic legs.

The measurement sessions were divided into four different trials (see figure 5.3, panel A). During the first and last trials, namely *Pre* and *Post* trials, the patients did not wear the robotic exoskeleton, as they were intended to measure their basal state and potential immediate effects after using the robot. The second and third trials were randomly assigned to either allow unrestricted motion by mechanically decoupling the REFLEX's joint (*Free* trial) or to provide gait assistance according to the *Pattern* control strategy (*Active* trial). Resting periods of ten minutes at least were interleaved between trials.

Two different measurement sessions were proposed, namely *RampVel* and *RandomVel*, depending on the order of the commanded gait speed. The training session data determined the gait speed levels of each patient. Gait speed varied from the identified comfortable gait speed (vel_1) to the 75% of their maximum gait speed (vel_3), with an equidistant intermediate speed level (vel_2). Each trial involved two repetitions of each velocity, lasting 60s each, so a total of four epochs were performed at the same speed.

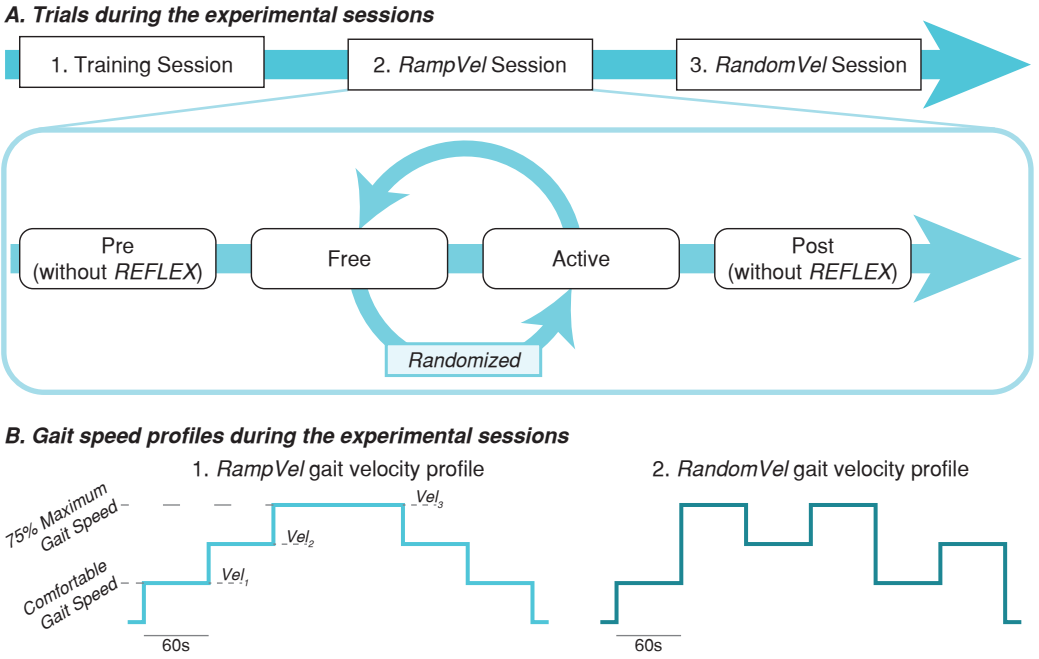

FIGURE 5.3: Description of the experimental protocol. Panel A shows the trials that composed each of the two experimental sessions. Panel B shows the gait speed profile used during both sessions. The gait speed varied on a patient-dependent scale from a comfortable level to 75% of the maximum tolerable speed in epochs of 60 seconds. During the *RampVel* session, the gait speed varied from the minimum to the maximum value and decreased afterward. Conversely, during the *RandomVel* session, the gait speed randomly varied using the same values as in the previous session.

In *RampVel* trials, gait velocity increased from the slowest to the fastest and returned to the slowest afterward. Conversely, the order of each velocity was randomly set in *RandomVel* trials. Panel B of figure 5.3 represents an example of the gait speed profile for a *RampVel* and a *RandomVel* trial. In these sessions, baseline EMG signals were recorded to determine the noise level of the sensors previously to carry out the trials.

A total of seven hemiparetic stroke patients were recruited for this study (demographic data is summarized in table 5.1). All of them gave their informed consent, and the study was conducted according to the Declaration of Helsinki after being approved by the local ethics committee.

5.3 Metrics and data analysis

Figure 5.4 represents an example of the raw data recorded during one trial. Raw information was segmented between consecutive heel strikes to divide it into steps and classified according to the commanded gait speed. Step data were normalized from 0 to 100% of the gait cycle. Figure 5.5 shows an example of average step data for one patient.

Table 5.1: Stroke subject's demographic data

Id Subject	***P1***	***P2***	***P3***	***P4***	***P5***	***P6***	***P7***	***Average***[a]
Age	57	63	63	68	56	56	57	60±4.69
Heigth (m)	1.7	1.8	1.7	1.7	1.7	1.7	1.8	1.74±0.05
Weigth (kg)	84	84	83	74	81	76	76	79.71±4.27
Time after stroke (months)	9	26	38	21	49	43	8	27.71±16.22
MMSE Score	29	27	13	26	26	25	29	25±5.51
FIM Score	117	104	79	118	90	107	126	105.86±16.61
Time Up and Go (s)	24.66	28.07	37.52	20.86	29.62	18.35	7.46	23.79±9.54
Sex	Male	Male	Male	Female	Male	Female	Male	
Stroke	Subcortical ischemic	Cortical ischemic	Cortical ischemic	Cortical hemorrhagic	Cortical hemorrhagic	Cortical hemorrhagic	Cortical hemorrhagic	
Paretic Side	Right	Left	Right	Right	Left	Right	Left	

[a]Mean±STD

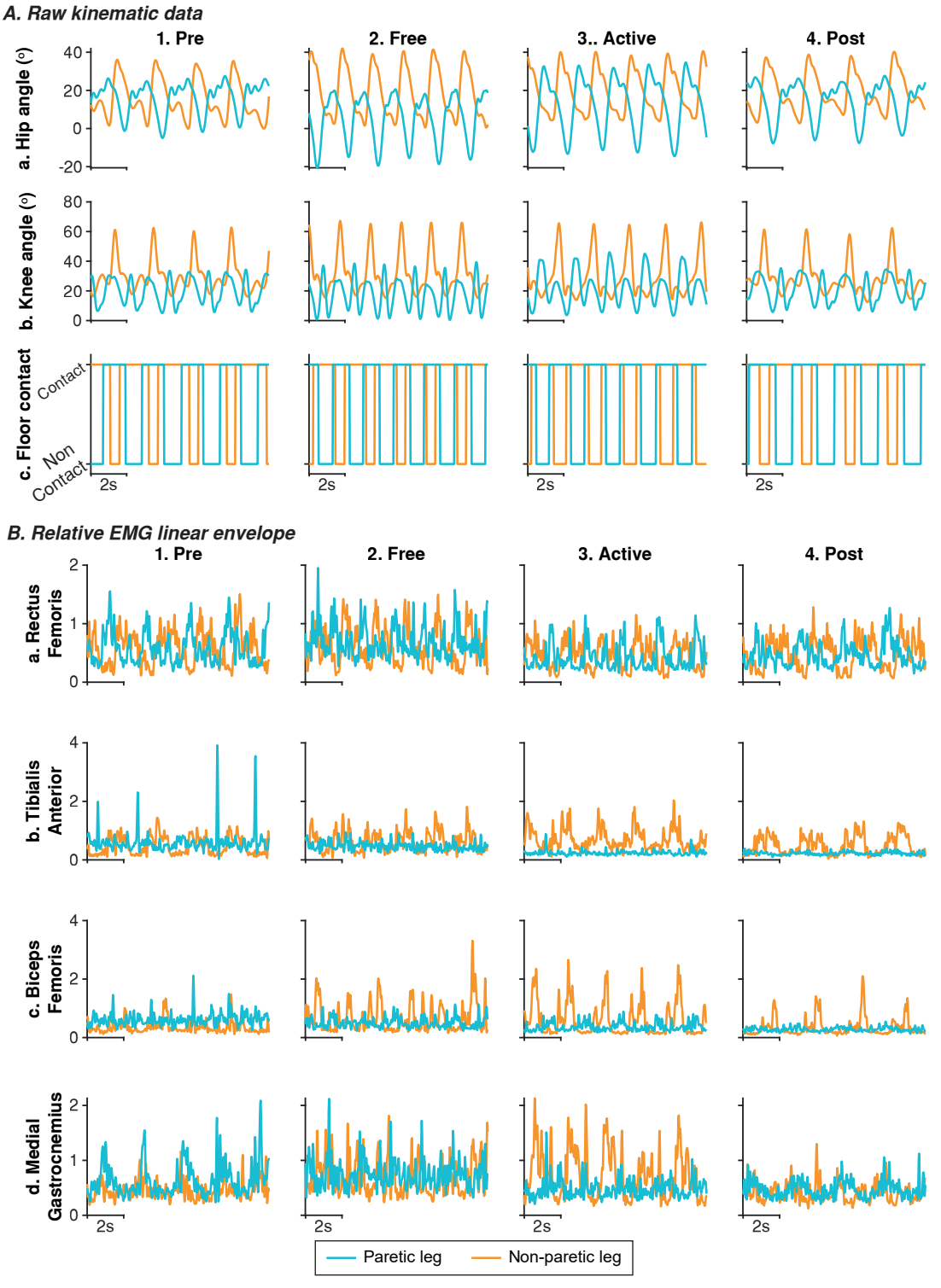

FIGURE 5.4: Example of raw data during an experimental trial. Panel A includes the flexion movements of hips and knees and the foot's contact with the floor. Panel B includes the linear envelope of the EMG signals after normalizing to the 95th percentile of the activity during the *Pre* trial. Both panels show information about the paretic and non-paretic legs through the cyan and orange lines, respectively

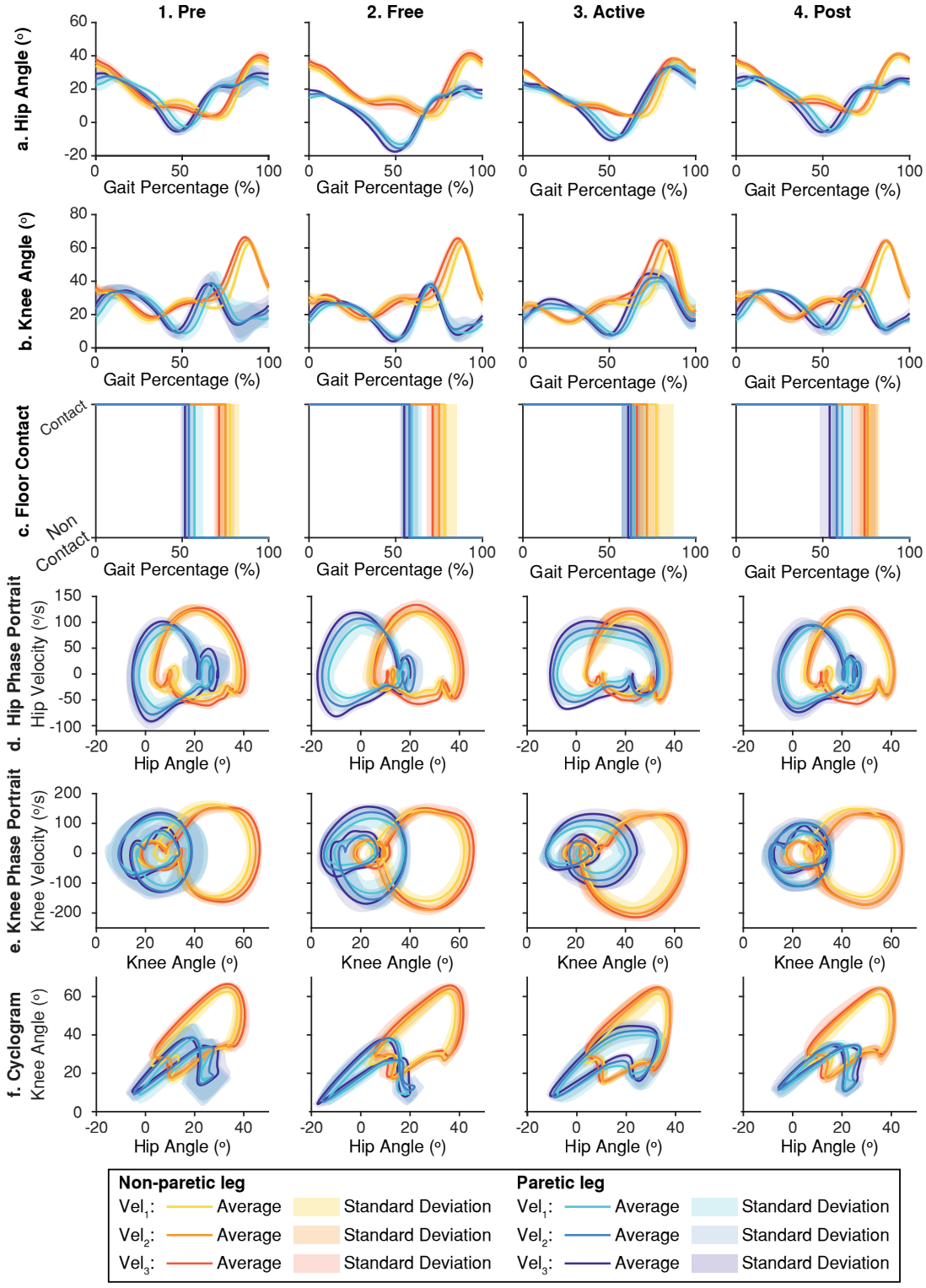

FIGURE 5.5: Example of step average kinematic data for one patient. Columns 1-4 represent the results obtained during each trial (*Pre*, *Free*, *Active* and *Post* trials respectively). Each row shows different kinematic information: hip and knee flexion angle (rows a and b), contact of the foot with the floor (row c), hip and knee phase portraits (rows d and e), and the hip-knee cyclogram (row f). The information of each leg and gait velocity is represented using a different color; solid lines represent the average data while semi-transparent areas represent the dispersion of the data (see the legend for details).

A threefold analysis was conducted with the recorded information. Its purpose was to assess the gait adaptation to the provided assistance and the embodiment of this technology. Concretely, gait features symmetry, motion kinematics, and muscular activity were evaluated.

5.3.1 Assessment of gait features symmetry

Four gait features were selected for this analysis: step length, step time, step velocity and stance/swing ratio (defined as the ratio between stance time and swing time, equation 5.1).

$$St/Sw(\%) = \frac{T_{stance}}{T_{swing}} \cdot 100 \tag{5.1}$$

The symmetry of these metrics was assessed using the Symmetry Index introduced in the previous chapter (equation 4.3). Figure 5.6 represents the distribution of these metrics for one example subject and their symmetry indexes.

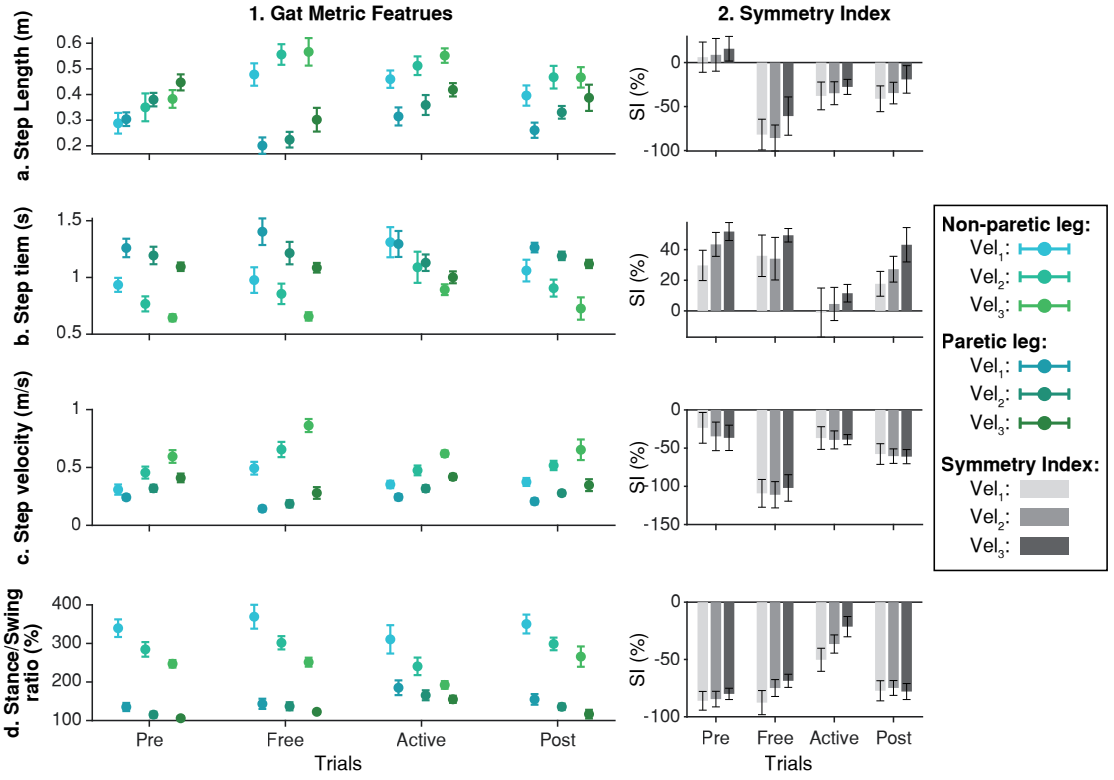

FIGURE 5.6: Example of gait feature metrics for one patient. Rows a-d show the information for different gait features: step length, step time, step velocity, and stance/swing ratio, respectively. Column 1 represents the metric distribution (mean +/- standard deviation) for each leg and gait speed across trials (see the legend for details). Column 2 represents the symmetry index of each gait metric across trials and gait speeds.

5.3.2 Assessment of motion kinematics

This analysis is based on the hip and knee phase portraits and the hip-knee cyclograms. Cyclograms show the hip flexion angle on the X-axis against the knee flexion angle on the Y-axis. The similarity between two motions was assessed using the similarity index defined in the equation 3.19 of the previous chapter. Although initially developed for phase-portraits representations, it is also applicable in other closed-shape figures such as cyclograms.

Figure 5.7 represents the results of comparisons between limbs motion for one patient. Two aspects were assessed: inter-limb and intra-limb similarity. Inter-limb similarity refers to the comparison between both legs within the same trial. In contrast, intra-limb similarity refers to the comparison between the motion of one leg during any trial and the same leg during the *Pre* trial. In this way, it is possible to find changes in the motion symmetry and identify the origin of these changes. For example, in figure 5.7, the knee phase-portrait shows an increase in inter-limb motion similarity, being these changes due to the evolution of both legs' motion since the comparison between *Pre* and *Active* trials showed differences in both legs.

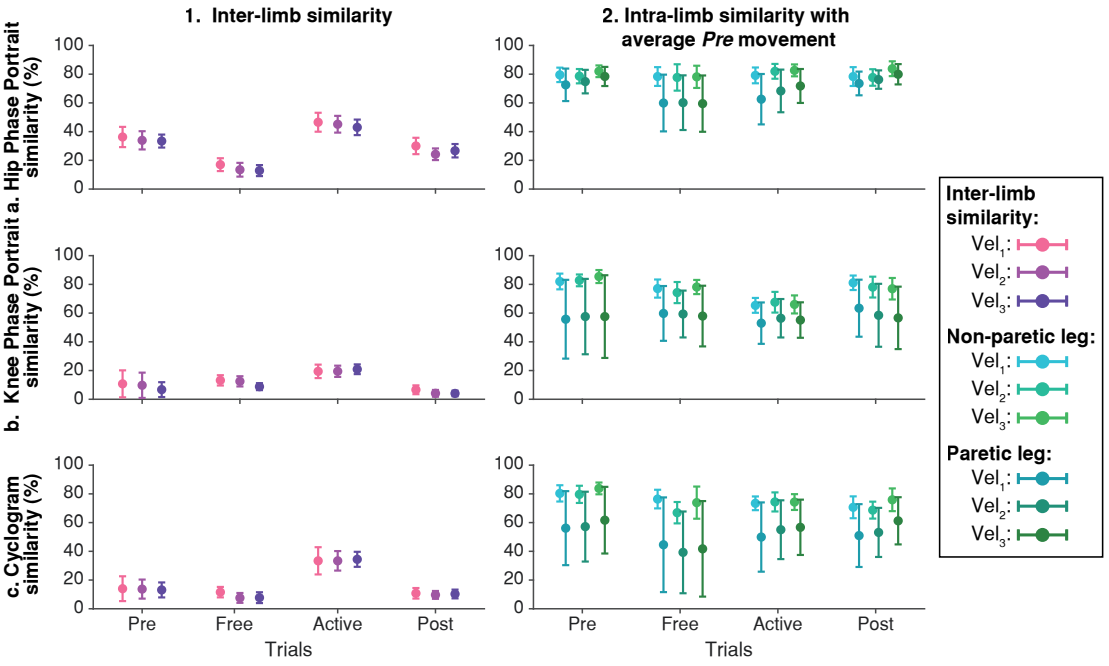

FIGURE 5.7: Example of inter-limb and intra-limb motion similarity in one patient. Columns 1 and 2 show the inter-limb motion similarity and the intra-limb motion similarity with the average motion during *Pre* trials. Data distributions are represented through the mean +/- the standard deviation. Rows a-c show the hip phase portrait, knee phase portrait, and cyclogram similarity, respectively. All the information is represented across trials and gait velocity (see the legend for more details).

5.3.3 Assessment of muscular activity

Two aspects were analyzed in the patients' muscular activity: amplitude and timing. The magnitude of this signal was assessed using its linear envelope ($leEMG$). In order to calculate it, Notch filters were used to remove electromagnetic environmental noise at 50Hz and harmonics; afterward, EMG signals were high-pass filtered (zero-lag 4th order Butterworth, cut-off 20Hz), rectified, and low-pass filtered (zero-lag 4th order Butterworth, cut-off 10Hz). Figure 5.8 represents an example of the average EMG linear envelope for one patient during the gait cycle. Two patients' Biceps Femoris EMG data had to be removed due to erroneous recordings and improper interactions between the electrodes and the robotic exoskeleton.

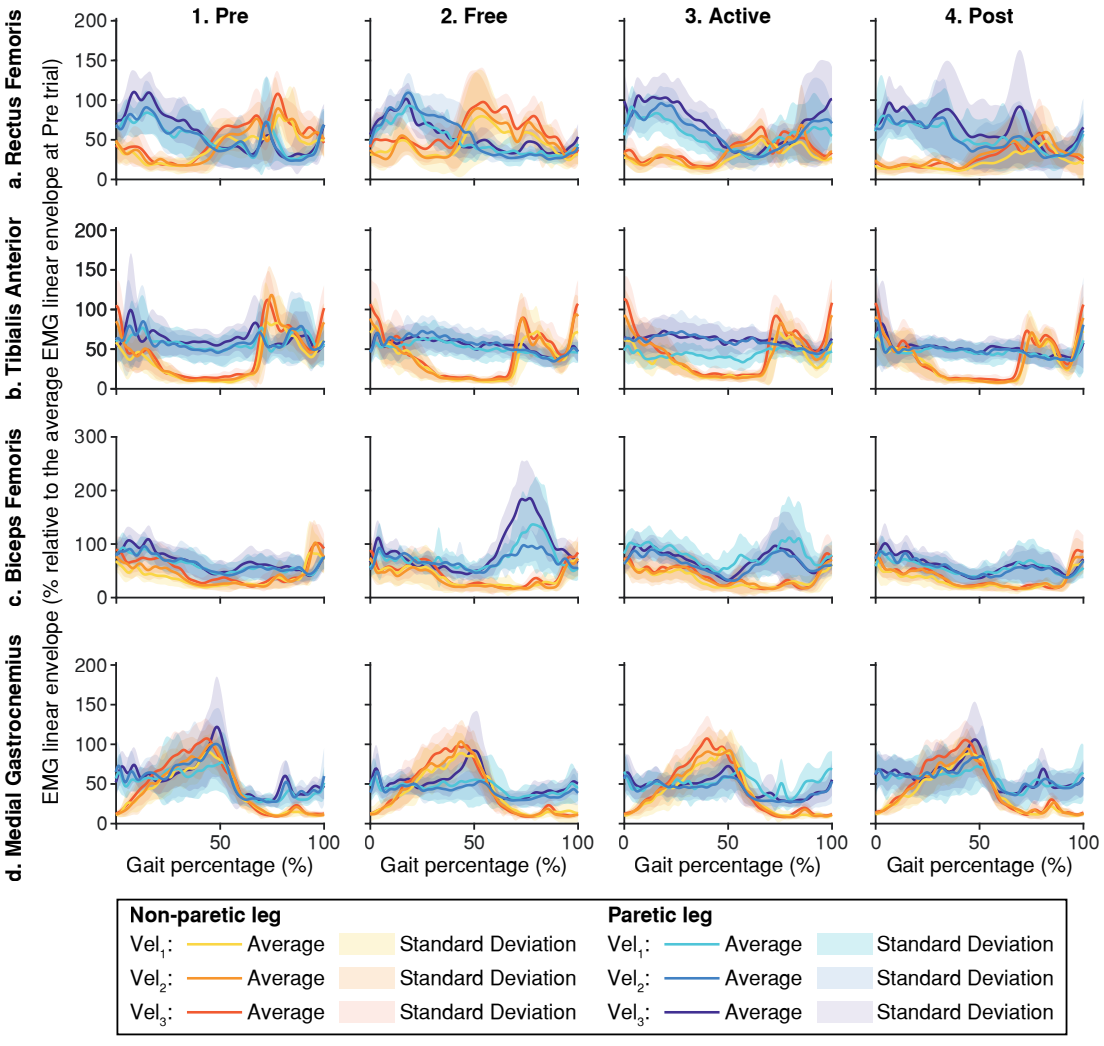

FIGURE 5.8: Example of average EMG linear envelopes for one patient. Columns 1-4 represent the results obtained during each trial (*Pre*, *Free*, *Active* and *Post* trials respectively). Each row shows the activation of a representative muscle: Rectus Femoris, Tibialis Anterior, Biceps Femoris, and Medial Gastrocnemius for rows a-d. The information of each leg and gait velocity is represented using a different color; solid lines represent the average data while semi-transparent areas represent the dispersion of the data (see the legend for details).

The magnitude of the muscular activity was assessed using the EMG Time Integral ($iEMG$) within a step, i.e. the area under the linear envelope (equation 5.2).

$$iEMG = \frac{\int leEMG}{T_{step}} dt \tag{5.2}$$

These measurements were normalized to the average $iEMG$ during the *Pre* trials. The relative $iEMG$, also called EMG ratio (RT_{EMG}) (equation 5.3), was defined to enable the comparison between trials and subjects and to determine the effects of the robotic assistance. Figure 5.9 represents an example of the relative EMG distributions for one patient across trials.

$$RT_{EMG}(\%) = \frac{iEMG}{\overline{iEMG}_{Pre}} \cdot 100 \tag{5.3}$$

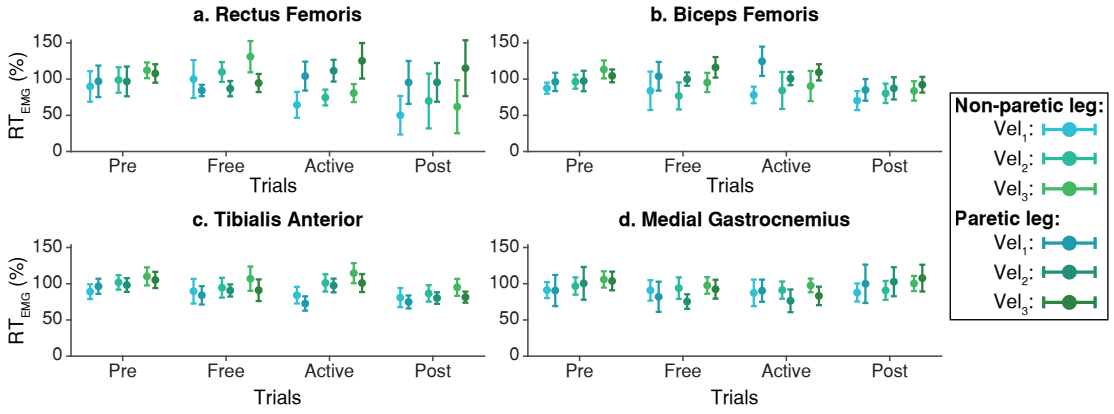

FIGURE 5.9: Example of muscular activity amplitude for one patient. Data distributions are represented through the mean +/- the standard deviation. Each panel represents information for a representative muscle: Rectus Femoris, Tibialis Anterior, Biceps Femoris, and Medial Gastrocnemius for rows 1-4. All the information is represented across trials and gait velocity (see the legend for more details).

The timings of EMG signals were evaluated using the Burst Duration Similarity Index ($BDSI$) [10, 282]. This metric compares the activation and inhibition periods of two EMG signals. To determine these activity periods, the Teager Kaiser Energy Operator (TKEO) was used to amplify instantaneous energy changes and differentiate between active and relaxed conditions [10, 335]. The noise signals acquired during the baseline recordings were used to determine the activation threshold. It was defined as fifteen times the standard deviations over the average baseline signal [335]. Figure 5.10 represents an example of EMG activation for one patient across trials. If a muscle is active in more than 50% of the steps in a certain step phase, this muscle is considered to be active at this phase.

Given two signals s_1 and s_2, of N samples, the BDSI between them requires two binary vectors: On_{EMG} and Off_{EMG}, with '1' indicating simultaneous activation or inactivation respectively and '0' otherwise. The BDSI is calculated according to equation 5.4 [10].

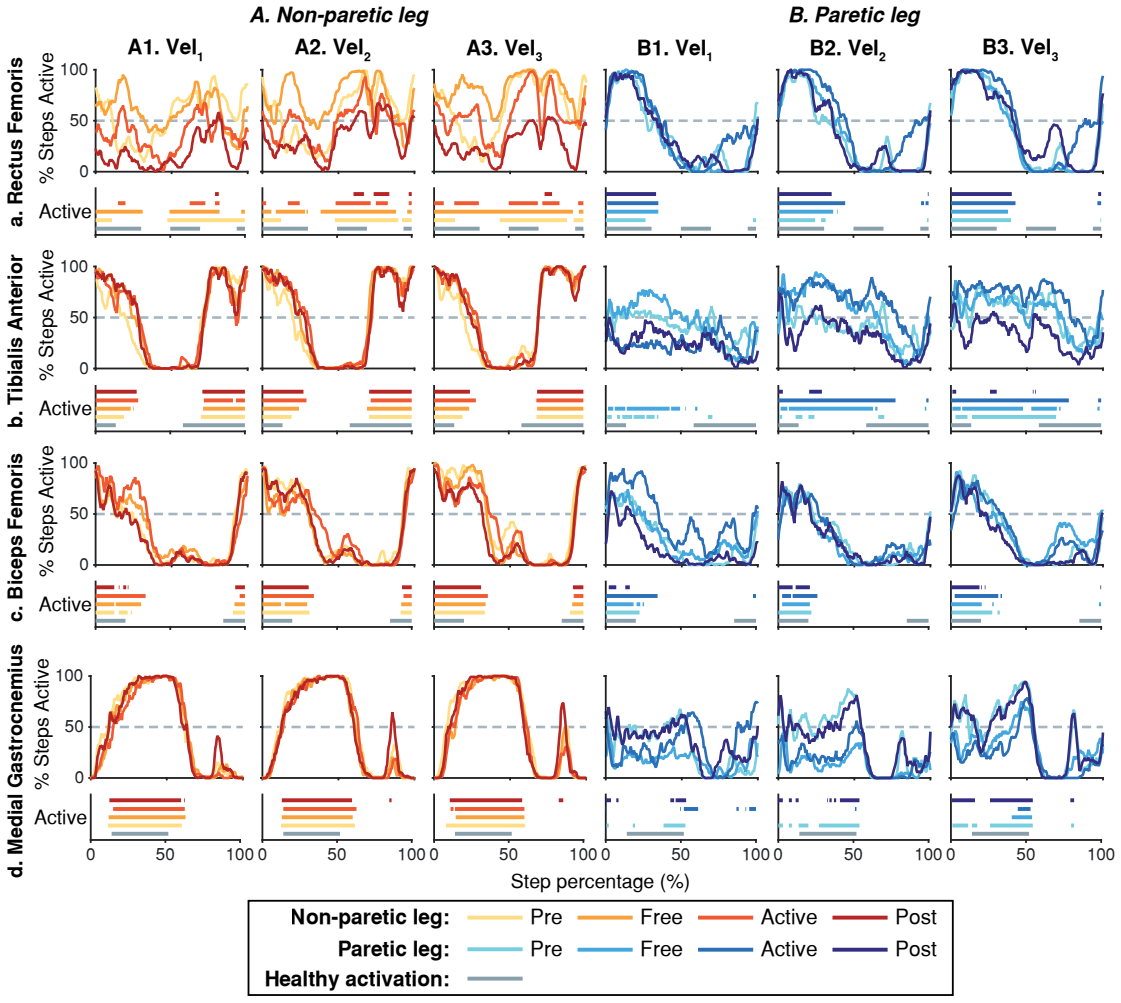

FIGURE 5.10: Example of average muscular activation for one patient. If the muscular activity is above the identified threshold, the muscle is considered to be active. Each panel is divided into two subplots; the upper represents the percentage of the total steps in which the muscle is active across a gait cycle, and the lower represents the average activation periods across a gait cycle and compares them with normal healthy timing (grey data). Columns A1-A3 and B1-B3 represent the obtained results during trials performed at the same velocity (namely vel_1, vel_2 and vel_3) and for the non-paretic (a's columns) and paretic legs (b's columns) respectively. Each row shows the activation of a representative muscle: Rectus Femoris, Tibialis Anterior, Biceps Femoris, and Medial Gastrocnemius for rows a-d. The information of each leg and trial is represented using a different color and gray lines represent healthy activation [251] (see the legend for more details).

$$BDSI(\%) = f(s_1, s_2) = \frac{sum(On_{EMG}) + sum(Off_{EMG})}{N} \cdot 100 \tag{5.4}$$

Timing analysis compared the muscular activation across trials with healthy activation patterns during normal-velocity gait extracted from [251]. Figure 5.11 represents an example of the BDSI distributions for one patient across trials.

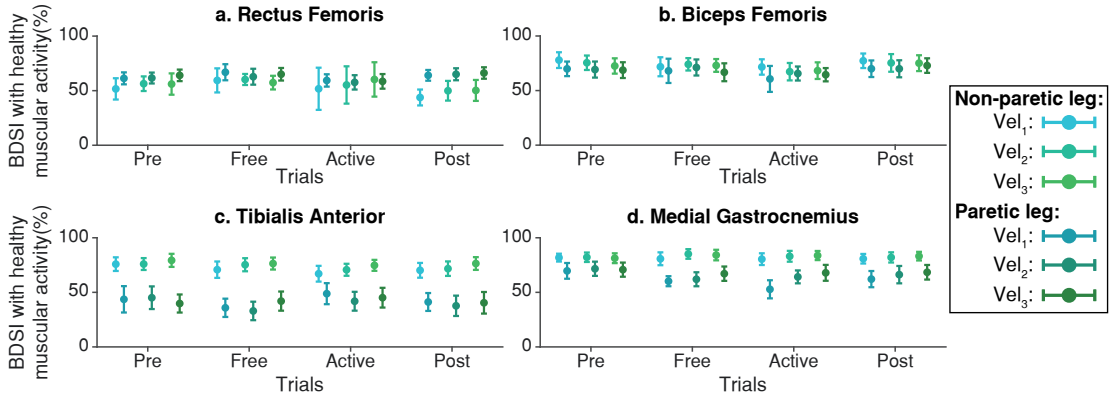

FIGURE 5.11: Example of muscular activity timing compared with healthy data for one patient. Data distributions are represented through the mean +/- the standard deviation. Each panel represents information for a representative muscle: Rectus Femoris, Tibialis Anterior, Biceps Femoris, and Medial Gastrocnemius. All the information is represented across trials and gait velocity (see the legend for more details).

5.3.4 Inter-subject analysis

Once the data of each patient was processed, a global analysis was conducted in order to find significant effects in all subjects due to the assistance provided by the robot. The metrics' distributions during a trial were built as follows: the average value during each velocity epoch for each patient was considered, so each patient was represented by four repetitions of the metric. After checking the heteroscedasticity (Levene test; $P < 0.05$) and non-normality (Kolmogorov-Smirnov test; $P < 0.05$) of some of the data distributions, significant differences between experimental conditions were looked for (Friedman test; $P < 0.05$). The Bonferroni correction was used to counteract the effect of multiple comparisons.

Figures 5.12-5.16 represent the distribution of the assessed metrics during vel_1, including gait features, kinematic analysis and muscular recruitment. However, none of these analysis resulted in significant effects due to robot assistance. Comparisons between different gait speeds did not result in significant differences in the metrics either. Figures C.1-C.5 in appendix C show these distributions for vel_2 and vel_3.

5.3.5 Intra-subject analysis

Although this experimental validation did not result in significant global effects due to REFLEX assistance, intra-subject analyses were conducted to evaluate individual changes in any of the evaluated metrics. The objective was to detect individual effects due to the robot's action, similarly to those obtained in the previous experiment (see chapter 4).

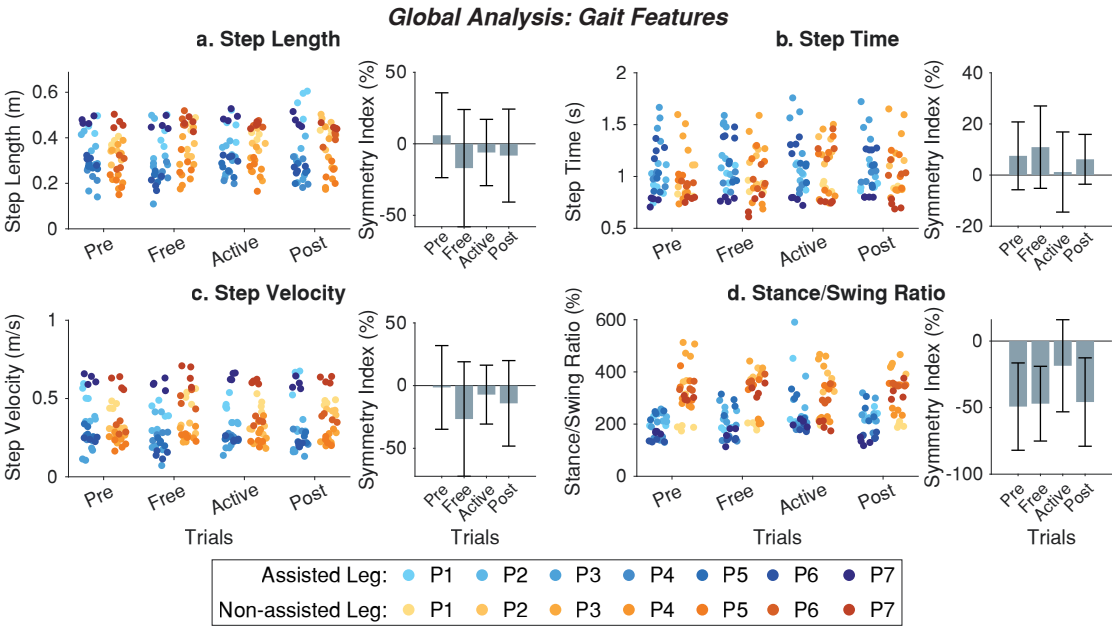

FIGURE 5.12: Global inter-subject gait features analysis at vel_1. Each panel (a-d) is divided into two subpanels: the left subpanel represents all the metric measurements differentiating trial, leg, and patient, while the right subpanel represents the symmetry index distributions across trials. The bar plot shows the average value +/- the standard deviation; markers represent individual metric values. The same color represents the same patient across the figure (see the legend for details).

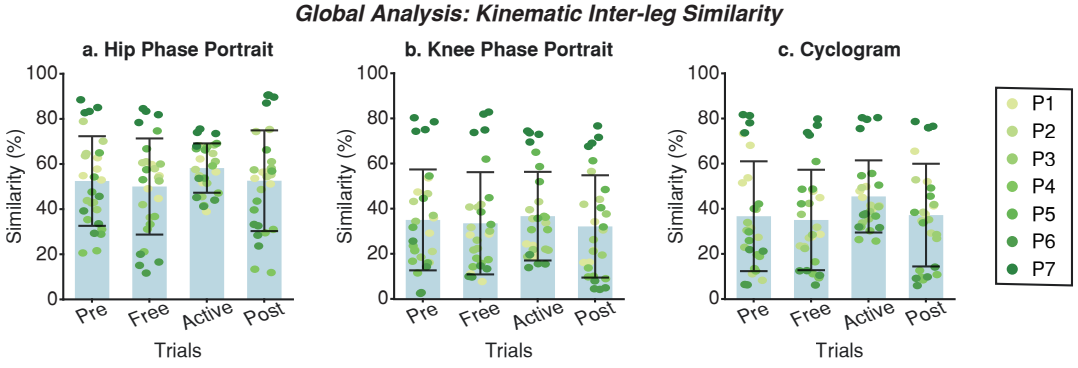

FIGURE 5.13: Global inter-subject analysis of interleg kinematic similarity at vel_1. Each panel (a-c) represents the interleg kinematic similarity across trials regarding the Hip phase portrait (a), the knee phase portrait (b), or the hip/knee cyclogram (c). The bar plot shows the average value +/- the standard deviation; markers represent individual metric values. The same color represents the same patient across the figure (see the legend for details).

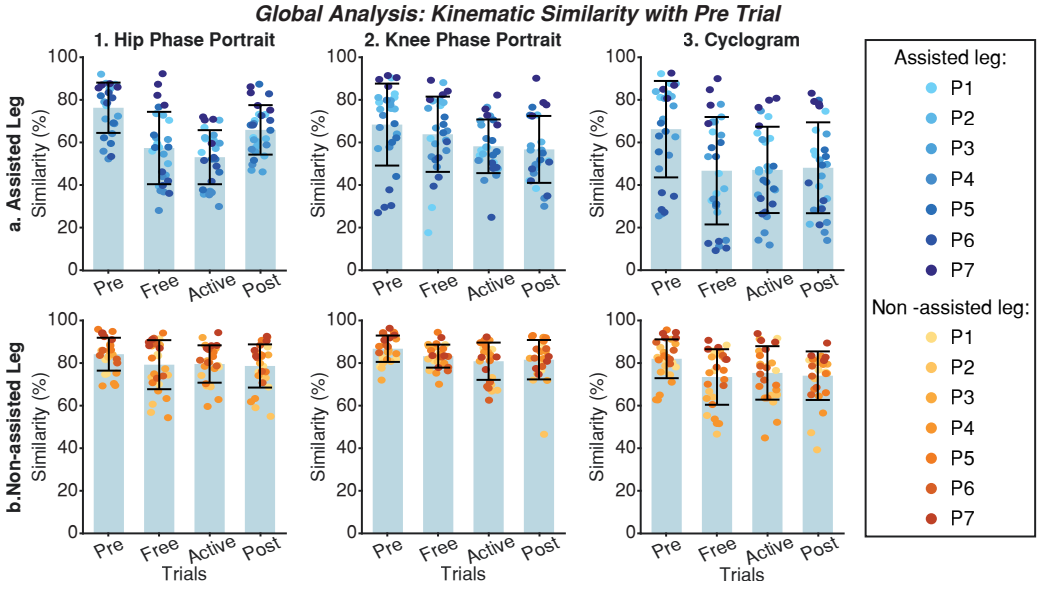

FIGURE 5.14: Global inter-subject kinematic intra-leg similarity analysis at vel_1. Each panel compares the evolution of kinematic representations from *Pre* across trials. Columns group the results of hip phase portraits (column 1), the knee phase portraits (column 2), and hip/knee cyclograms (column 3). The first row represents the metric for the assisted leg, while the second row represents the non-assisted leg. The bar plot shows the average value +/- the standard deviation; markers represent individual metric values. The same color represents the same patient across the figure (see the legend for details).

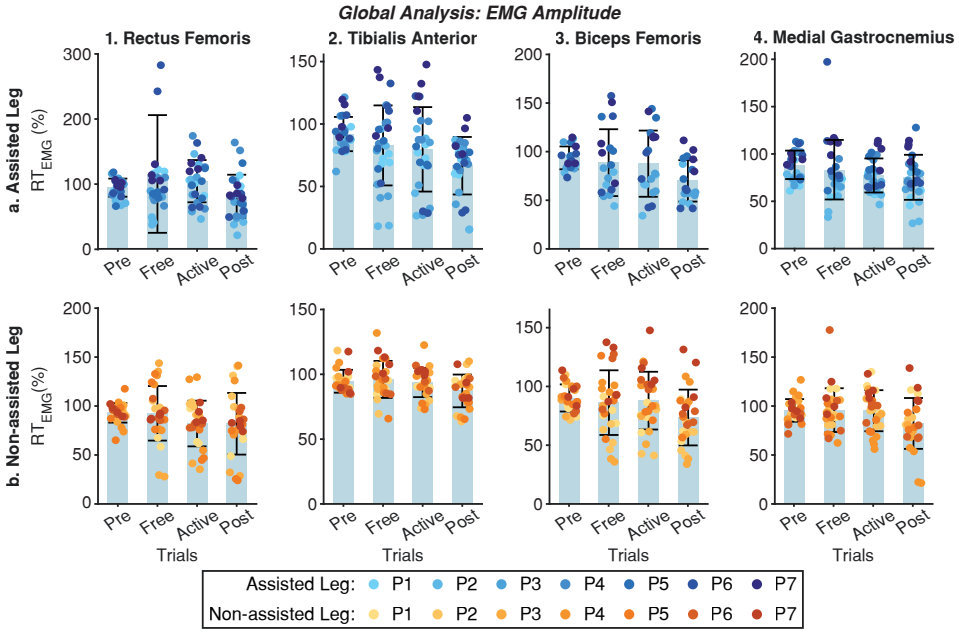

FIGURE 5.15: Global inter-subject EMG amplitude analysis at vel_1. Each panel represents the relative EMG amplitude compared with *Pre* across trials. Columns group the results for the same muscles (Rectus Femoris, Tibialis Anterior, Biceps Femoris, and Medial Gastrocnemius for columns 1-4), and rows group data for the same leg (assisted and non-assisted leg in the first and second row, respectively). The bar plot shows the average value +/- the standard deviation; markers represent individual metric values. The same color represents the same patient across the figure (see the legend for details).

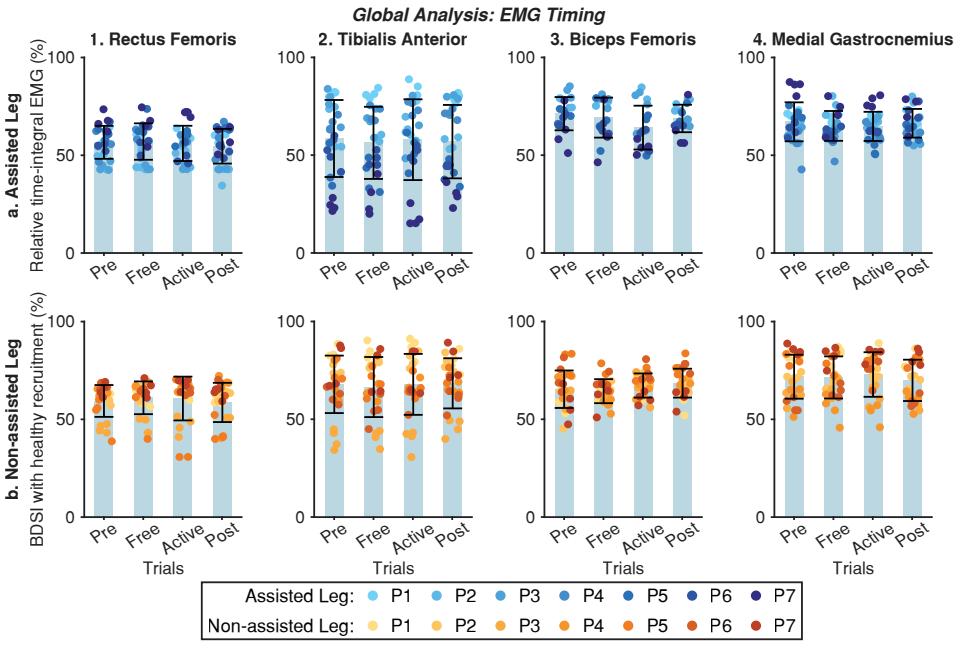

FIGURE 5.16: Global inter-subject EMG timing analysis at vel_1. Each panel represents the BDSI with the normal healthy muscular recruitment across trials. Columns group the results for the same muscles (Rectus Femoris, Tibialis Anterior, Biceps Femoris, and Medial Gastrocnemius for columns 1-4), and rows group data for the same leg (assisted and non-assisted leg in the first and second row, respectively). The bar plot shows the average value +/- the standard deviation; markers represent individual metric values. The same color represents the same patient across the figure (see the legend for details).

The data distributions that characterized each trial and gait velocity were built by pooling together the assessed metrics during each step at the evaluated trial and velocity. The statistical analyses were performed across trials for each gait velocity. Normality (Kolmogorov-Smirnov test; $P > 0.05$) and homoscedasticity (Levene test; $P > 0.05$) of the distributions involved were assessed. If they were fulfilled, ANOVA tests were used for determining significant differences between distributions ($P < 0.001$); otherwise, Kruskal-Wallis tests were used ($P < 0.001$). In both cases, Bonferroni corrections were used to deal with the effect of multiple comparisons. Since global results were not found, this analysis was limited to immediate effects; therefore, only *Pre*, *Free* and *Active* trials were compared.

Figures 5.17-5.21 summarize the individual results of this analysis for each patient during vel_1. Figures C.6-C.10 in appendix C show these individual results for vel_2 and vel_3. As it can be seen, although there are significant differences between trials within a patient, all patients did not response in the same way and even some of them presented contrary behaviors, showing an increase or a decrease of the same metric under the same conditions.

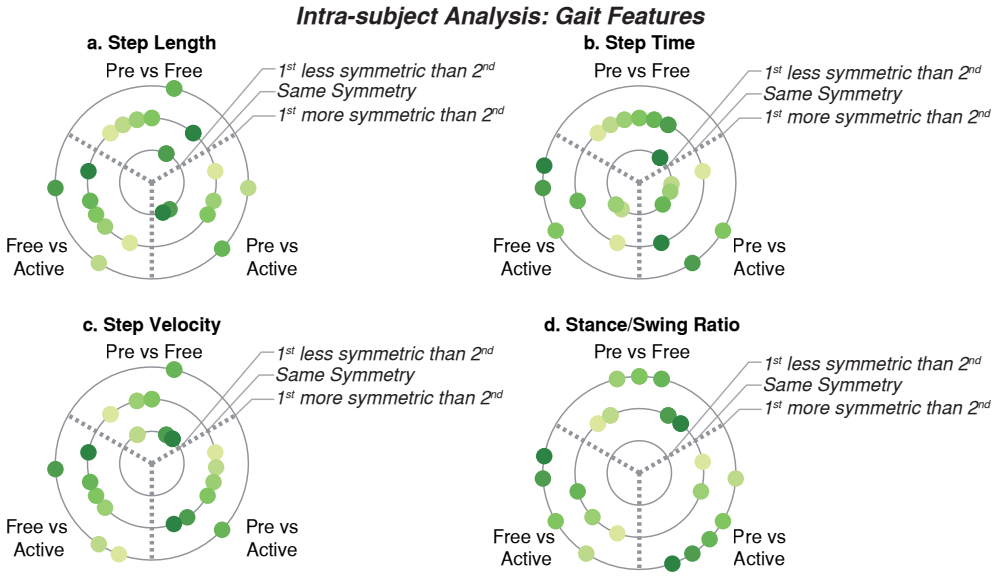

FIGURE 5.17: Summary of the intra-subject gait feature analysis at vel_1. Each panel (a-d) represents the results when comparing the symmetry of a gait feature between *Pre*, *Free* and *Active* trials. Each subject is represented with a different color and the same color represents the same patient across panels.

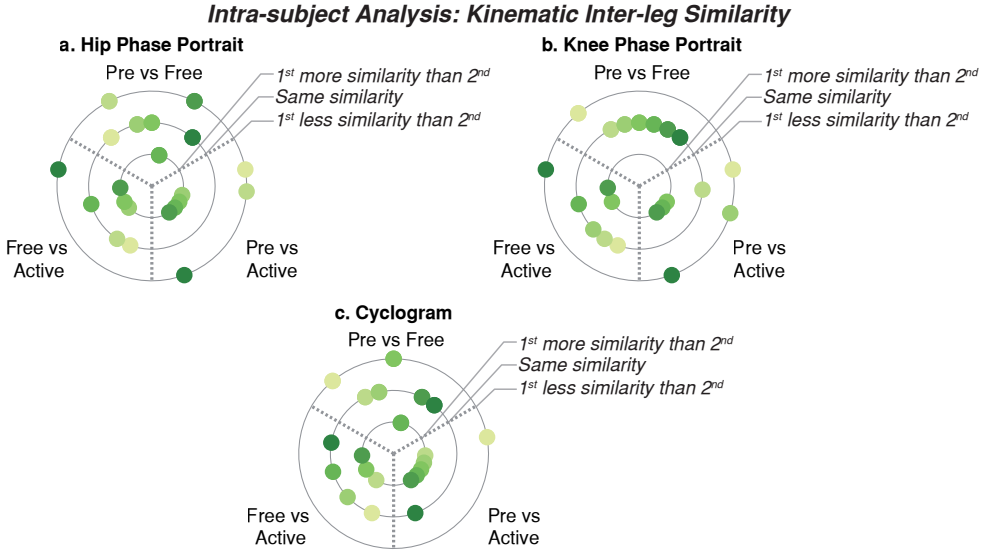

FIGURE 5.18: Summary of the intra-subject kinematic inter-leg similarity analysis at vel_1. Each panel (a-c) represents the results when comparing the similarity between limbs of different kinematic representations between *Pre*, *Free* and *Active* trials. Each subject is represented with a different color and the same color represents the same patient across panels.

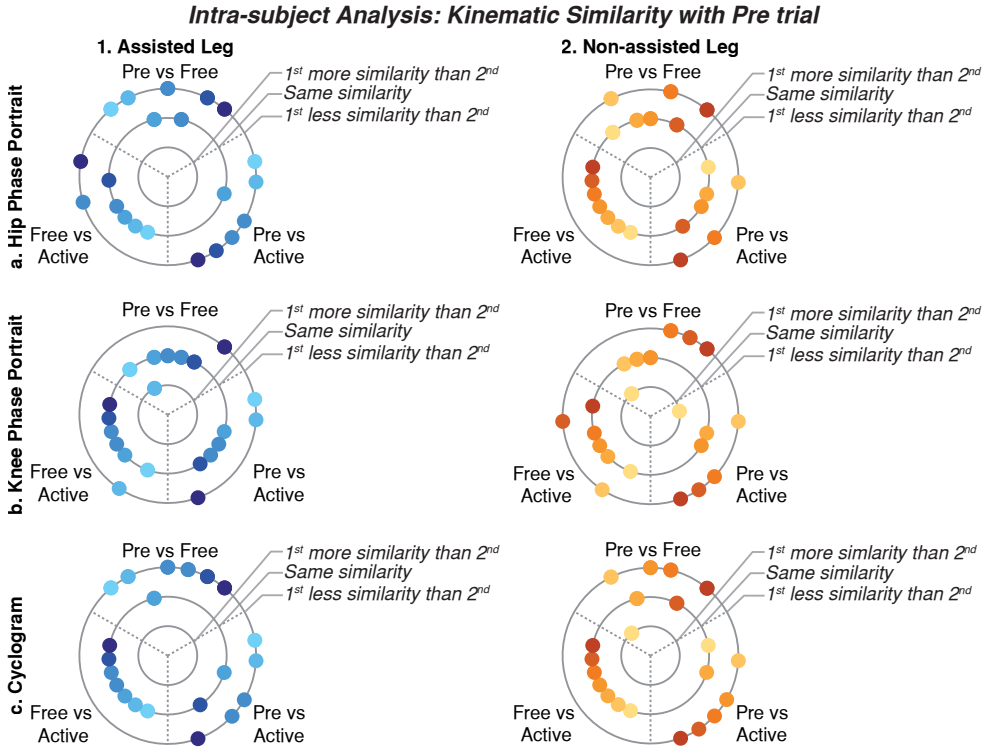

FIGURE 5.19: Summary of the intra-subject kinematic intra-leg similarity analysis at vel_1. Each panel represents the evolution of kinematic representations from *Pre*, they also compare this evolution in *Pre*, *Free* and *Active* trials. Columns group the results for the same leg (assisted leg in the column 1, and non-assisted leg in column 2). Rows group results for the same kinematic representations (hip phase portrait, knee phase portrait and cyclogram for rows a-c). Each subject is represented with a different color, the same brightness gradation represents the same patient across panels.

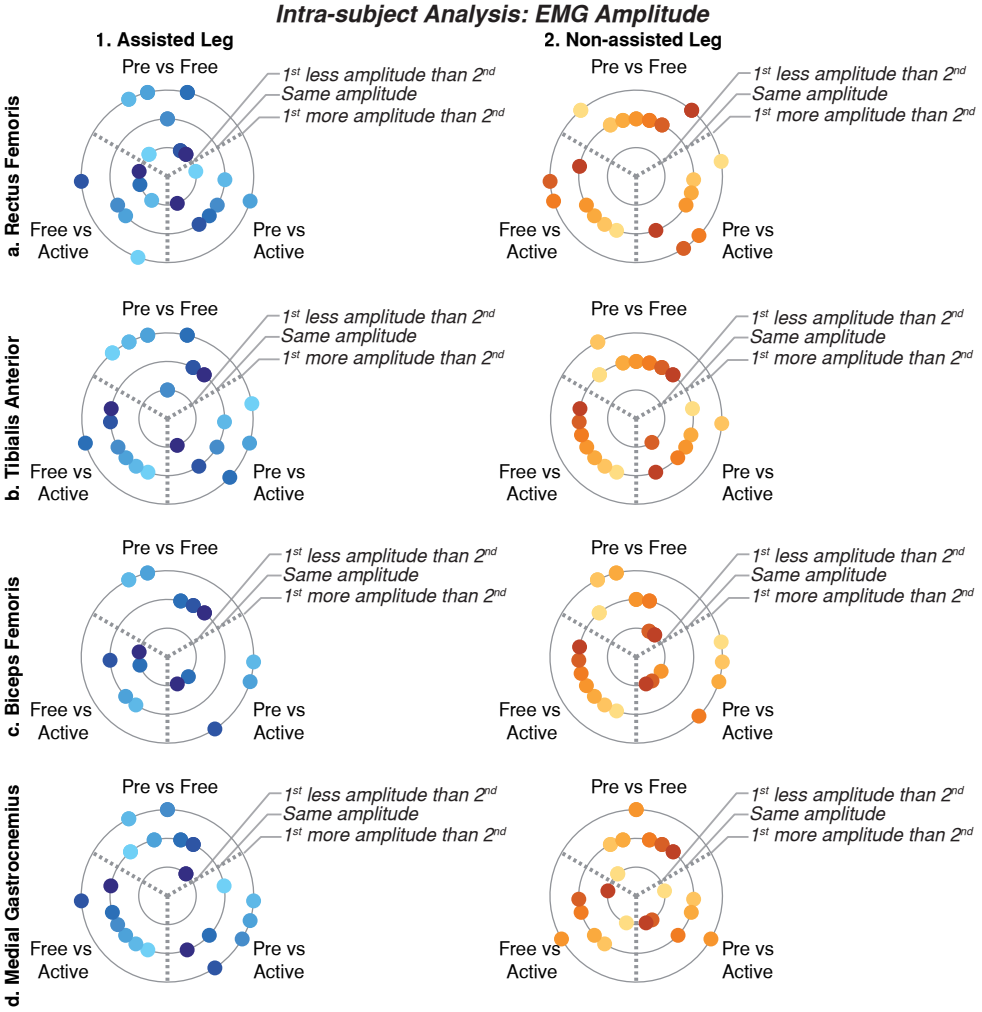

FIGURE 5.20: Summary of the intra-subject EMG amplitude analysis at vel_1. Each panel compares the EMG amplitude for different muscles between *Pre*, *Free* and *Active* trials. Columns group the results for the same leg (assisted leg in the column 1, and non-assisted leg in column 2). Rows group results for the same muscles (Rectus Femoris, Tibialis Anterior, Biceps Femoris and Medial Gastrocnemius for rows a-d). Each subject is represented with a different color, the same brightness gradation represents the same patient across panels.

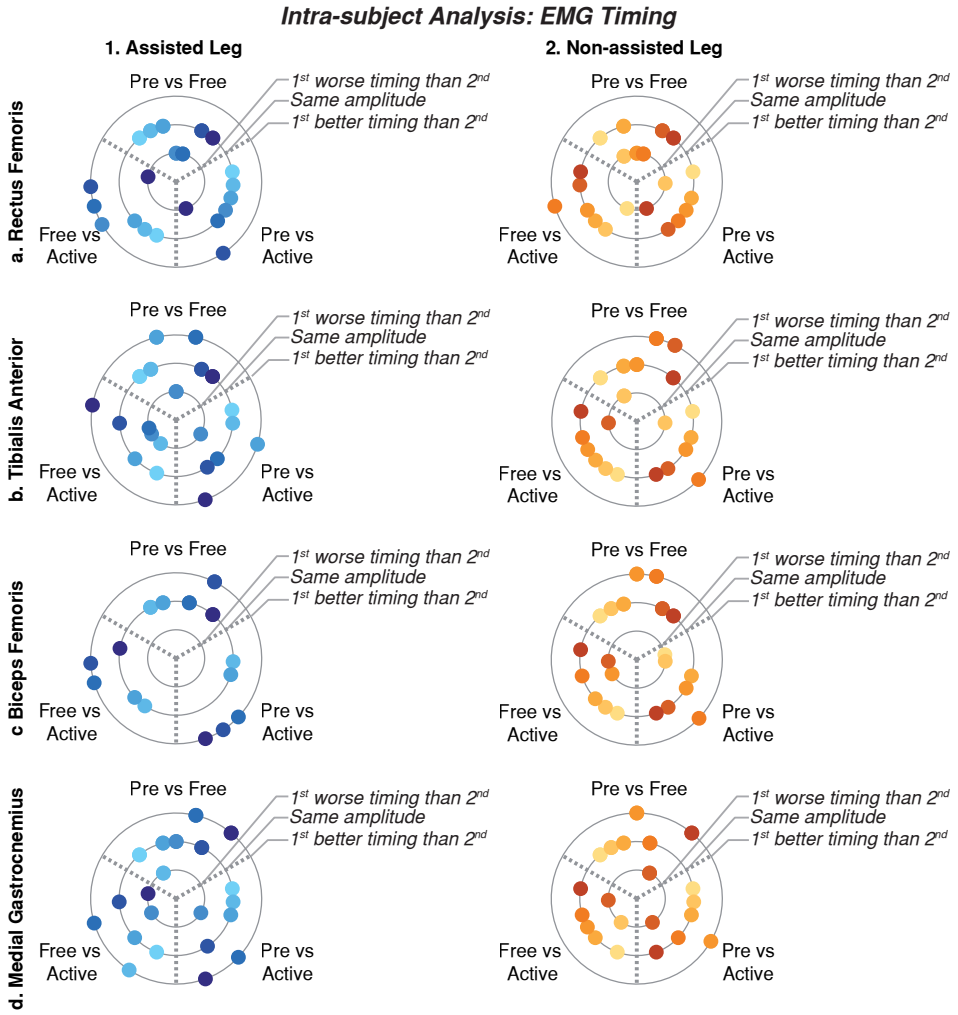

FIGURE 5.21: Summary of the intra-subject EMG timing analysis at vel_1. Each panel compare the BDSI calculated respect to healthy activation for different muscles between *Pre*, *Free* and *Active* trials. Columns group the results for the same leg (assisted leg in column 1 and non-assisted leg in column 2). Rows group results for the same muscles (Rectus Femoris, Tibialis Anterior, Biceps Femoris, and Medial Gastrocnemius for rows a-d). Each subject is represented with a different color, the same brightness gradation the same patient across panels.

For instance, step length symmetry or step time symmetry responded differently to robot assistance, as some patients increased these symmetries while others decreased them. Another example of different subjects' behavior is the muscular response to assistance, independently of the muscle or leg assessed.

5.3.6 Sample size for significant results

In order to evaluate the statistical power of the inter-subject analysis, the sample sizes required to detect significant differences that would validate the hypothesis were calculated. Using the sample size calculation proposed by Kadam et al. [164], sample sizes were calculated to obtain significant differences with a 95% significance and 80% power according to the data variation and average changes obtained during this pilot experiment. Tables 5.2-5.6 summarize the required sample sizes for each assessed metric.

All the metrics evaluated (excepting the hip phase-portrait intra-leg similarity) would require a larger sample size to detect significant effects due to REFLEX assistance. This is because of the high variance of the results. The high inter-subject variability observed requires a larger sample size to ensure the significance of the obtained effects due to robot assistance so that the initial hypothesis can be accepted or rejected.

TABLE 5.2: Sample size for significant gait feature effects

Gait Velocity	**Step Length**	**Step Time**	**Step Velocity**	**Stance/Swing Ratio**
Vel_1	65.65	822.38	2225.28	12.60
Vel_2	69.22	558.74	200.76	8.50
Vel_3	62.14	2391.78	395.37	7.97

TABLE 5.3: Sample size for interleg kinematic effects

Gait Velocity	**Hip Phase Portrait**	**Knee Phase Portrait**	**Cyclogram**
Vel_1	94.06	2504.22	81.74
Vel_2	82.14	1653.46	76.39
Vel_3	53.13	5078.20	43.65

5.4 Discussion on the embodiment of REFLEX assistance

Based on the preliminary validation results, this study was conducted involving a higher number of patients to reinforce the hypothesis of this dissertation. Increasing the number of measured subjects revealed new results that were not observed in the

TABLE 5.4: Sample size for intraleg kinematic effects

Gait Velocity	***Paretic Leg***			***Non-paretic Leg***		
	Hip Phase Portrait	**Knee Phase Portrait**	**Cyclogram**	**Hip Phase Portrait**	**Knee Phase Portrait**	**Cyclogram**
Vel_1	3.27	15.05	10.51	43.54	35.70	49.88
Vel_2	2.10	13.20	7.76	114.34	36.88	19.25
Vel_3	1.88	15.89	6.51	12.06	12.54	7.75

TABLE 5.5: Sample size for muscular amplitude effects

Gait Velocity	***Paretic Leg***				***Non-paretic Leg***			
	Rectus Femoris	**Tibialis Anterior**	**Biceps Femoris**	**Medial Gastrocnemius**	**Rectus Femoris**	**Tibialis Anterior**	**Biceps Femoris**	**Medial Gastrocnemius**
Vel_1	59.33	77.49	11.17	9.38	15.17	458.97	121.42	246.80
Vel_2	18.86	89.25	209.42	4.33	4.91	124.82	5677.86	1415.05
Vel_3	52.86	100.21	70.03	20.64	26.51	285.41	6620753.273	319.62

TABLE 5.6: Sample size for muscular timing effects

Gait Velocity	***Paretic Leg***				***Non-paretic Leg***			
	Rectus Femoris	**Tibialis Anterior**	**Biceps Femoris**	**Medial Gastrocnemius**	**Rectus Femoris**	**Tibialis Anterior**	**Biceps Femoris**	**Medial Gastrocnemius**
Vel_1	2611.62	21395.04	11.09	357.63	205.27	235.72	150.75	106.35
Vel_2	354.09	2096.96	45.86	437.58	1580.83	2278.95	243.18	474.27
Vel_3	110.48	636.53	8418.60	1034.88	3293.20	3347.87	8715.20	3482.99

previous validation. During the former experiment, results seemed to indicate that REFLEX's assistance could improve the gait symmetry in hemiparetic subjects or, at least, compensate for the disturbance introduced by the own device. However, during the current validation, the action of REFLEX was heterogeneous across patients since some of them improved their gait symmetry according to the gait metrics and the kinematic measurements, while others reported a less symmetric gait, reducing step length or step time symmetry or the inter-leg similarity of hip and knee phase portraits for instance.

Actually, during the current validation, the action of the robot assistance in the paretic knee movement was not as evident as during the preliminary experiment. This difference may be because the exoskeleton was better tailored for the first group of participants than for the second one. The prototype adjustment is limited, and a worse joint alignment, which results in worse force transmission, may be responsible for this poor exoskeleton's performance. According to Babic et al., this is a common problem in the field as joint alignment and efficient power transmission are key factors for the proper function of these devices [15].

The main outcomes obtained from this experiment were the high variance and heterogeneous behaviors of all the evaluated metrics, which emphasizes the singularities of each patient to cope with the provided assistance. This high dispersion is present not only in the metrics related to the muscular activity, as previously reported in [2], but also in the kinematic and gait metric results. The main consequence of this variability was that no global effects were identified due to REFLEX assistance. Although the metrics showed a positive evolution due to assistance during the preliminary validation, this behavior could not be extrapolated to the group. However, the sample size used during the experiment does not allow us to reject the hypothesis either (see section 5.3.6).

Despite significant group effects not being detected, it does not mean that REFLEX assistance had no effects on the patients. Actually, significant effects were identified at the subject level but were not consistent among them. All the evaluated metrics showed significant positive effects in one subject at least; however, contrary effects were also reported. This discrepancy and heterogeneous responses reinforce the necessity of properly tailoring the robot to each patient individually to adapt the exoskeleton to each subject and therefore maximize its performance [2]. The high variance in the attained results is also responsible for not being able to accept neither reject the hypothesis, since a larger sample size would have been necessary.

A plausible explanation for this high variance in the measured outcomes might be the varying conditions of the experiment. The experimental protocol was based on the results of Haufe et al. [135], who reported kinematic and muscular adaptation after one minute of using a knee exoskeleton. However, they recruited healthy subjects instead of stroke survivors. Stroke consequences in the nervous system may require longer adaptation periods to the robot action.

Longer trials without velocity changes would imply more stable experimental conditions that would favor reaching the gait's steady-state and, therefore, reduce the variance of the measured outcomes. This improvement in the experimental procedure would also facilitate the integration of the robot assistance by the patient, i.e., its embodiment, since repetitiveness improves matching the patient's expectation and robot's action. These aspects will be addressed in future experiments.

Muscular reactions were not homogeneous across patients either. Some of them reduced muscular activation amplitude while others increased it or did not show any variation, independently of whether the assessed leg was the assisted or the unassisted one. Similarly, recruitment timing responses were heterogeneous, remaining unchanged, increasing or decreasing the timing similitude with the healthy activation indistinctly.

In this sense, our initial hypothesis was that the assistance provided by REFLEX would lead to variations in muscular activity and compensatory strategies. However, although some significant variations were identified for individual subjects, no global effects were found. This contrasts with the results of previous experiments, where the assistance provided by a robotic exoskeleton reduced the activity of the involved muscles [125, 195, 337, 338, 340, 379]. However, it is necessary to remark that all these previous experiments were conducted with healthy subjects instead of stroke survivors.

Schmalz et al. reported a reduction in the compensatory strategies developed by hemiparetic subjects due to the assistance of a knee robotic exoskeleton [313]. However, none of the six patients involved in the study had suffered a stroke, but their hemiparesis was due to different underlying conditions. Another previous study involved stroke survivors and reported muscular changes [352], although the authors carried out a complete rehabilitation therapy and the reported muscular variations were after it. Therefore these changes are not only due to the assistance but also due to the therapeutic effect of the intervention.

Androwis et al. also reported muscular adaptation in stroke patients during a unique simulated therapy session [10]. Their results showed a significant increase in muscular activity in the Rectus Femoris and Soleus of the paretic leg and better activation timing for the affected Vastus Lateralis and Rectus Femoris. Although muscular reactions were reported in this case, two main differences are present compared with the presented approach. On the one hand, they used the EksoGT prototype, a complete lower-limb robotic exoskeleton for gait training, instead of a single-joint knee exoskeleton. On the other hand, their purpose was gait rehabilitation instead of gait assistance. In this regard, they looked for a higher muscle involvement in the paretic leg instead of reducing compensatory strategies and muscular activity in the nonparetic leg.

Although some of the participants involved in this REFLEX validation showed significant effects in their muscular recruitment, these were not correlated with kinematics

modifications. This fact indicates that the kinematic variations are more likely due to the biomechanic effect of the extra load and the forces exerted by REFLEX than to the integration of the REFLEX's actions by the Nervous System. If these actions had been properly embodied, the nervous system would have modified the muscular activity in consequence, but this adaptation did not occur.

When comparing the reported results in the published literature and those obtained in this experiment, although the conclusions seem to be opposed, there is an important difference that it is necessary to highlight. The above-mentioned articles that reported a reduction in the compensation mechanisms or the proper integration of the assistance while walking did not involve stroke patients but healthy or hemiparetic walking subjects with a different underlying condition.

Stroke may directly affect the integration of afferent signals by the CNS, leading to proprioception deficits in several cases [109, 291]. Actually, the motor-learning ability of a subject depends on their central proprioceptive processing [371]. This proprioceptive impairment due to stroke may also be a reason for the different effects between healthy and stroke populations when assisted by a robotic exoskeleton. If the CNS is not able to properly process the afferent information that reports the device's action, it is not possible for the CNS to react appropriately in consequence. However, if this integration occurs exclusively at the spinal level, which remained unaffected due to stroke, our hypothesis would be valid, and the robot's assistance would lead to the reduction of compensatory mechanisms. Research efforts are needed in this regard, so the ability of stroke survivors to detect and process the assistive action of the robot would be fully understood.

5.5 Conclusions

This chapter has presented the second experimental validation carried out with the REFLEX prototype involving stroke survivors. The aim of this validation was to confirm the results obtained during the preliminary study and further understand how stroke survivors integrate the robot's actions. However, the high dispersion of the obtained metrics avoided confirming or rejecting the original hypothesis.

Although global assistance effects were not identified, significant effects were reported at the subject level. Each subject responded differently to the assistance, highlighting the necessity of properly tailoring the robot controller to each patient individually. Notably, differences were found between how the assistance affected the stroke patients that participated in this study and how healthy subjects responded to robotic assistance, according to other studies reported in the literature. More research is needed to

understand the implications of the stroke's consequences in how patients acquire the action of robotic exoskeletons and if they are able to integrate it properly.

Chapter 6

CONCLUSIONS AND FUTURE DIRECTIONS

This final chapter presents the main contributions and the principal conclusions of this doctoral thesis. Likewise, it exposes future work lines based on the reached conclusions. Eventually, the scientific publications derived from this dissertation are listed as an index of its scientific quality.

6.1 Contributions

The main aim of this doctoral thesis was to assist post-stroke hemiparetic gait through the embodiment of a partial robotic exoskeleton. In this regard, this thesis covers the required technical developments and the experimental validation of such an approach. The work methodology followed by the author started with an analysis of the related scientific literature. Healthy and post-stroke gait were analyzed to establish the assistive strategy to be followed. Likewise, robotic alternatives to assist hemiparetic gait were considered. Following this analysis, the author defined the following starting hypothesis:

- Post-stroke gait is not only characterized by muscular weakness and motor control deficits in the paretic leg but also by compensatory strategies developed in the non-paretic leg to achieve a functional and stable gait. These compensations are partially responsible for the high metabolic cost of hemiparetic walking, and for secondary musculoskeletal pathologies in the nonparetic limb.
- Actuating over the paretic leg directly assists the affected joint function, promoting a more stable and symmetric gait. This assistance may reduce compensation strategies because it targets their origin. If the assistance is able to decrease the

deficits of the paretic leg, the compensation mechanisms should also decrease since they would not be required.

- A partial robotic exoskeleton is particularly suitable for this purpose for two main reasons. Firstly, it allows reduced size and weight, minimally disturbing the user's gait, and its action can be focused on the paretic joint function. Secondly, since the non-paretic leg is not assisted, it is possible to observe the effects on the sound leg without acting over it.
- In order to reduce post-stroke compensation mechanisms, the action of the robotic exoskeleton should be properly integrated by the Nervous System. Since the device would not act on the non-paretic leg, the decrease in its compensatory strategies would be due to the Nervous System modifying the gait pattern and muscular recruitment. In other words, the reduction of compensatory strategies would be fully achieved if the exoskeleton is embodied by the user.
- Partial robotic exoskeletons have been widely used to assist human locomotion in healthy subjects. Several studies have reported muscular adaptations and metabolic cost reduction due to the assistance provided by these robots. This fact points out that the Nervous System properly integrated the action of these devices since muscular recruitment and kinematic gait patterns evolved to those less demanding for these subjects by leveraging the action of the robotic device.
- The embodiment of a robotic device relies on the reliable and predictable timing of its action in such a way that it matches the user estimation. In the case of a partial robotic exoskeleton, this issue is especially challenging since the timing of its action relies on its control algorithms to be actively coordinated with the current user gait.

The work collected in this dissertation followed an iterative process of deepening into the state-of-the-art of robotic gait assistance, developing technological solutions, and assessing its performance. The main contributions of this thesis are summarized below:

- Exposition of an extensive review of control strategies to coordinate the action of partial robotic exoskeletons and human gait. These strategies were analyzed, and their weaknesses and strengths were highlighted. Experimental validation procedures of these devices were also reported to evaluate the differences between those focused on healthy or impaired subjects. This work is exposed in the chapter 1 of this document and in the review article [217].
- Application of an Extended Kalman Filter to estimate sagittal joint axis and lower limb motion during gait in unsupervised environments based on accelerometer and gyroscope data. This development is described in the chapter 2 of this document and published in the research article [216].

- Assessment of the above-mentioned sensory system to control partial wearable robotic devices following the two most extended synchronization strategies: FSM and AFOs. This is exposed in the chapter 2 of this document and in the research paper [216].
- Development and validation of two control strategies for partial robotic exoskeletons to naturally assist hemiparetic gait based on the movement of the non-paretic leg. This technical development is described in the chapter 3, in the conference proceeding [219] and the research paper [218] (under peer-review with minor revisions required, preprint available).
- Development of the REFLEX knee exoskeleton to provide robotic gait assistance through the proposed strategies. It was described in the chapter 4 of this document, in the conference proceeding [219], and in the research article [218] (under peer-review with minor revisions required, preprint available).
- Preliminary validation of the proposed assistive strategies with healthy subjects and stroke survivors. Gait adaptations were specially assessed, and results seemed to point out the correct integration of the robot assistance in hemiparetic patients since the gait pattern of the non-assisted leg evolved to a healthier movement. These results were described in the chapter 4 of this document, and in the research paper [218] (under peer-review with minor revisions required, preprint available).
- Evaluation of the REFLEX assistance in a larger cohort of hemiparetic subjects. On this occasion, muscular activity was also evaluated in both legs to evaluate if the provided assistance was able to modify the muscular recruitment. This validation was discussed in the chapter 5 of this dissertation and is part of a publication in preparation.

6.2 Embodiment of the REFLEX exoskeleton in perspective and future work

In the initial stage of this doctoral work, the author was focused on reviewing the scientific literature to deepen into the causes and characteristics of hemiparetic gait as well as the effects of assisting human gait through a robotic exoskeleton. Two primary outcomes from this review led to the basis of the hypothesis. On the one hand, hemiparetic gait characteristics are not only direct consequences of brain damage but also of compensation mechanisms that arose to deal with such direct impairments. On the other hand, partial robotic exoskeletons are able to generate assistance that is properly integrated by the Nervous System of healthy users, leading to changes in muscular recruitment and kinematic gait patterns that are less demanding for the users.

Based on these two facts, the author aimed to assist the paretic joint functions because if this assistance is integrated, the compensatory strategies that arose in the non-paretic limb to deal with gait impairments would not be required and, therefore, should decrease. To achieve this objective, the work was then oriented to the technological developments required to test the hypothesis.

The embodiment of a robotic exoskeleton depends on the timing of its action. The users will integrate its assistance if it is provided according to their estimations. However, partial robotic exoskeletons require to be actively coordinated with human gait through their control algorithms. The first development of this doctoral work was a sensory system based on gyroscope and accelerometer data that monitors human gait and can be used as input for such algorithms.

The proposed system is able to estimate the axis of the sagittal movements of lower-limb joints in real-time. Since the axis estimation is calculated while walking, calibration or set-up procedures are unnecessary. The system is also able to deal with sensor displacements while walking since such axes are computed continuously. This feature enables the proposed approach to be used in unsupervised environments while performing daily life activities. This approach was evaluated with healthy subjects while walking, obtaining similar results to those previously reported. It was also evaluated as input of partial exoskeleton controllers. Errors and delays remained under the required thresholds; therefore, the system was validated as a source of gait features for such algorithms. Since control timing was considered to be properly managed, this sensory system is suitable for promoting the embodiment of a robotic exoskeleton.

This dissertation then proposed a control paradigm for unilateral exoskeletons to naturally assist hemiparetic gait and looking for the proper integration of such assistance by the Nervous System. Such a paradigm was based on the fact that the movement of both legs is delayed half-step while walking. In this regard, it is possible to use the motion of the non-paretic leg to establish the timing of the assistance as well as to define kinematic features of the provided assistive pattern. Two assistance strategies were proposed: replicating the movement of the non-assisted leg or synchronizing a healthy gait pattern.

The REFLEX prototype is then presented as the platform to evaluate the performance of the mentioned assistive strategies and their possible embodiment. It is a robotic knee exoskeleton that reinforces the knee during the stance phase and guides its movement during the swing to promote gait symmetry. During its preliminary validation with healthy subjects, the system was proven to compensate for the disturbance introduced by the extra load of the device, showing a gait symmetry in these subjects similar to normal walking without the device.

When hemiparetic subjects were involved in the experiment, the assistance provided by REFLEX promoted their gait symmetry, especially when assisting by providing a healthy gait pattern, since all patients showed a more symmetric gait in this case. Interestingly, the symmetry improvements were not only due to modification in the paretic gait kinematic, but the non-assisted leg motion also evolved to become similar to the healthy pattern provided. These results pointed out a proper integration of the assistance by the Nervous System since it generated a different gait pattern in the non-assisted limb.

The promising results of this preliminary validation motivated a second validation with a larger cohort of stroke patients (seven subjects) to confirm the hypothesis. The analyses of this validation were regarding kinematics, gait features, and amplitude and timing of muscular activity. The high dispersion of the measured outcomes prevented us from accepting or rejecting our hypothesis; however, significant effects were detected at the subject level. This different behavior for each subject highlights the necessity of adequately tailoring the assistance provided and the exoskeleton morphology to each subject's needs.

Importantly, although kinematics effects were detected due to robotic assistance, these were not correlated with changes in muscular activity. This pointed out that the kinematics effects were due to the effect of the extra load and torques exerted by the device instead of due to the device's embodiment.

A deep understanding of the neural mechanisms involved in the integration of assistive devices is required. If the neural structures involved in this process were affected by the stroke, this would hamper the proper acquisition and integration of the robot's action. In this regard, extra research efforts are needed to identify how healthy subjects and stroke survivors may integrate this information.

6.2.1 Future work lines

The work developed in the context of this doctoral thesis and the conclusions reached during the experimental tests have served the author to identify future work lines. Some of them are improvements of the device or the experimental procedures that arose after validating the prototype, while others are experimental trials to deepen into the understanding of co-adaptation between assistive exoskeletons and stroke survivors.

6.2.1.1 Improvement of REFLEX mechanical design and interface with the body

The morphology and mechanical design of the REFLEX prototype should be improved to ensure the proper assistance delivery to the users. The REFLEX design was based on previous rehabilitation exoskeletons, but it resulted in a heavy device that is not optimized for gait assistance. A new design that ensures a lighter device and maintains torque supply is encouraged to leverage the potential of the proposed assistive strategies.

It would also be desirable to increase the number of actuated joints. The system could provide more complete assistance if it was able to actuate also over the hip and the ankle. The assistive strategies proposed in this document can be directly extrapolated to new joint movements, and thus, the device could be suitable for a broader range of patients.

To ensure that the assistance is properly provided, the interface of the exoskeleton with the user's body should be improved. A new tailoring system that can be adaptable to different users and ensures the correct joint alignment with the actuator axis would boost the assistive potential of the device.

6.2.1.2 Simpler experimental protocols for more reliable results

The high dispersion of the results obtained during the second experimental validation may be partially attributed to the changing velocity conditions during the trials. Although the evaluation of the adaptation process to variable gait speed was an objective of this experiment, this changing condition artificially increased the variability of the measured outcomes.

Simplifying the experimental protocol by reducing gait speed variability should lead to more reliable outcomes with less variance. This new protocol would also ensure that the gait steady-state is being assessed. During the original protocol, subjects may have never reached the gait steady-state after each speed variation; instead, they might remain in consecutive transient states.

This new protocol would ensure static experimental conditions and allow the isolation of the assistance effects from reactions due to the changing gait speed. In this regard, more reliable results should be obtained, allowing the proper evaluation of the technology embodiment.

6.2.1.3 Further analysis of the embodiment of assistive technology

The experiments carried out in the framework of this doctoral thesis are a first approximation to understanding the embodiment of robotic exoskeletons in stroke survivors. Further experimentation is required to elucidate the aspects that still remain elusive about this phenomenon.

Extra analysis can be carried out to directly measure the embodiment of a robotic exoskeleton, following the same methodology previously reported to assess the embodiment of prosthesis or wheelchairs [278]. In this regard, subjective questionnaires or personal interviews could be used to evaluate if users consider the device as a part of their own body [32, 33, 243, 264] or the proprioceptive drift could be measured as a direct and objective sign of a change in the body schema [76, 280, 312].

Research efforts should also be made to identify the neural structures involved in the embodiment of assistive tools in both healthy subjects and stroke survivors. The role of the afferent information acquired by the Nervous System should also be analyzed to identify the most relevant and, therefore, be able to ensure a proper sensory information delivery to the subject.

6.2.1.4 Hybrid interfaces for assistance integration

The embodiment of robotic devices requires that users perceive and integrate their actions. However, neurological patients may experiment some troubles acquiring this afferent information. In this regard, the assistive device should provide a twofold effect. It must exert torques and forces to mechanically assist the impaired gait, but it also should be enriched by afferent stimulation to ensure the acquisition of the exerted action.

New hybrid interfaces must be developed to ensure the proper delivery of this double action. Several approaches could be followed for these new neural interfaces. For example, they could be based on electrical stimulation, similar to those used in hybrid exoskeletons for gait assistance [8, 81] but remaining its intensity under the motor threshold to only provide sensory information. This strategy has been previously used in neuroprosthesis as a source of afferent stimulation to reduce tremor in Parkinson's Disease and Essential Tremor patients [94, 215].

A different alternative could be haptic interfaces based on vibrotactile stimulation, like those used to enhance the performance of rehabilitation robots [24]. This stimulation can be used to artificially trigger responses in muscular spindles and Golgi tendon organs to induce proprioceptive changes [294]. This afferent stimulation has been already validated to induce hand movements in healthy subjects as a consequence of their proprioception alteration [211].

This afferent feedback has been successfully developed for amputees to properly acquire sensory information about the interaction and movement of their active prostheses [285, 292]. Recently, non-invasive interfaces have also been used to improve the control of such prostheses through afferent feedback [26]. However, these strategies have not yet been used with neurological patients wearing an active orthosis.

The final objective of the proposed neuroprosthesis would be to artificially generate proprioceptive information to conceal sensory deficits in neurological patients. If this afferent information is properly synchronized with the robot's action, it could simulate the missing afferent information to completely acquire the action of the robotic device and promote its embodiment.

6.2.1.5 Exoskeleton assistance and embodiment assessment during daily life

The final purpose of assistive robotic exoskeletons is to use them in daily life. However, the REFLEX prototype was only validated in a supervised environment while walking over a treadmill. This prototype must also be tested in unstructured environments and during overground walking, especially validating the proposed control paradigm. This may allow the transition of the developed control paradigm to its implementation in active orthosis designed for daily use.

Further experimental tests must be carried out to ensure that the expected embodiment and adaptations also occur during overground walking. If this is confirmed, these results would also be extrapolated to daily life assistance. The real long-term embodiment of this technology should be assessed during longitudinal trials with stroke survivors receiving daily gait assistance. This would be the next step to definitely promote the use of robotic exoskeletons to assist impaired gait in daily life.

6.3 Scientific dissemination

6.3.1 Publications

This thesis has allowed the author to be involved in several research works, both technical and clinical. The following scientific contributions are an indicator of the work quality collected in this document.

6.3.1.1 Journal articles

- Lora-Millan, J. S., Moreno, J. C., and Rocon, E. (2022). Coordination Between Partial Robotic Exoskeletons and Human Gait: A Comprehensive Review on

Control Strategies. *Frontiers in Bioengineering and Biotechnology* 10, 842294 doi:10.3389/fbioe.2022.842294.

- Lora-Millan, J. S., Hidalgo, A. F., and Rocon, E. (2021). An IMUs-Based Extended Kalman Filter to Estimate Gait Lower Limb Sagittal Kinematics for the Control of Wearable Robotic Devices. *IEEE Access* 9, 144540–144554. doi:10.1109/ACCESS.2021.3122160.

- Lora-Millan, J. S., Sanchez-Cuesta F.J., Romero, J.P., Moreno J.C., and Rocon, E. (2022). A Unilateral Robotic Knee Exoskeleton to Assess the Role of Natural Gait Assistance in Hemiparetic Patients. *Journal of Neuroengineering and Rehabilitation*, under review.

- Di Natali, C., Chini, G., Totaro, M., Lora-Millán, J. S., Rocon, E., Beccai, L., et al. (2021). Quasi-Passive Resistive Exosuit for Space Activities: Proof of Concept. *Applied Sciences*. 11, 3576. doi:10.3390/app11083576.

6.3.1.2 Conference Proceedings

- Lora-Millan, J. S., Moreno, J. C., and Rocon, E. (2021). Estrategias para la asistencia a la marcha de sujetos con hemiparesia a través de una órtesis activa de rodilla, In *XLII Jornadas de Automática: Libro de Actas*, 91–98. doi:10.17979/spudc.9788497498043.091.

- Lora-Millan, J. S., Moreno, J. C., and Rocon, E. (2020). Assessment of gait symmetry, torque interaction and muscular response due to the unilateral assistance provided by an active knee orthosis in healthy subjects. In *2020 8th IEEE RAS/EMBS International Conference for Biomedical Robotics and Biomechatronics* (IEEE), 229–234. doi:10.1109/BioRob49111.2020.9224414.

- Hidalgo, A. F., Lora-Millan, J. S., and Rocon, E. (2019). IMU-Based Knee Angle Estimation using an Extended Kalman Filter. In *2019 41st Annual International Conference of the IEEE Engineering in Medicine and Biology Society (EMBC)* (IEEE), 570–573. doi:10.1109/EMBC.2019.8857614.

- Lora-Millan, J. S., and Rocon, E. (2019). Estrategias de control de un exoesqueleto robótico para la asistencia en la flexo-extensión de rodilla para pacientes con hemiparesia. In *2019 Iberdiscap. X Congreso Iberoamericano de Tecnologías de Apoyo a la Discapacidad* (Buenos Aires), 327–330.

- Lora-Millan, J. S., and Rocon, E. (2019). Desarrollo y validación de algoritmos de control de una órtesis activa de rodilla para sujetos hemiparéticos basados en la cinemática de la pierna sana. In *Jornadas Nacionales de Robótica - Spanish Robotics Conference* (Alicante), 21–28.

- Lora-Millan, J. S., Hidalgo Romero, A. F., and Rocon de Lima, E. (2018). Diseño de una Órtesis Activa para la evaluación de algoritmos de asistencia robótica en sujetos hemiparéticos. In *Actas de las XXXIX Jornadas de Automática*, Badajoz, 5-7 de Septiembre de 2018, 57–63.

6.3.2 International Experience

During this doctoral thesis, the author carried out a research visit awarded by the Spanish Ministry of Universities. During this abroad experience, the author worked in the Wearable Robotics Laboratory of the Biorobotics Institute of Scuola Superiore Sant'Anna (Pontedera, Italy) under the supervision of Dr. Nicola Vitiello.

During this three-month period, the author worked with a compliant hip exoskeleton to assist stand-to-sit transitions in stroke patients and with an EMG system to evaluate the performance of this task. This work enabled the author to use EMG information to assess task performance and was an opportunity to learn about a different approach to solving problems similar to those faced during this doctoral work.

6.3.3 Research lines collaborations

Apart from the research conducted in the framework of this dissertation, the author has also collaborated with other research lines during his PhD. He was involved in a project about the suppression of Essential Tremor through afferent stimulation and in a project about a robotic platform for hip fracture rehabilitation in elderly people. These collaborations also led to the scientific contributions that are listed below:

1. *Journal articles*

    - Lora-Millan, J. S., Delgado-Oleas, G., Benito-Leon, J., and Rocon, E. (2021). A Review on Wearable Technologies for Tremor Suppression. *Frontiers on Neurology* 12, 1–17. doi:10.3389/fneur.2021.700600.
    - Lora-Millan, J. S., Lopez-Blanco, R., Gallego, J. A., Mendez-Guerrero, A., Gonzalez de la Aleja, J., Rocon, E., et al. (2019). Mechanical vibration does not systematically reduce the tremor in essential tremor patients. *Scientific Reports*. 9, 16476. doi:10.1038/s41598-019-52988-8.

2. *Conference Proceedings*

    - Costa, V., Ramirez, O., Lora-Millan, J. S., Urendes, E., Rocon, E., Perea, L., et al. (2020). Design of a robotic platform for hip fracture rehabilitation in elderly people. In *2020 8th IEEE RAS/EMBS International Conference*

for Biomedical Robotics and Biomechatronics (BioRob) (IEEE), 599–604. doi:10.1109/BioRob49111.2020.9224320.

- Lora Millan, J. S., Lopez Blanco, R., Gallego, J. A., Gonzalez de la Aleja, J., and Rocon, E. (2019). La estimulación mecánica aferente no reduce sistemáticamente el temblor de pacientes con temblor esencial. in *Libro de Actas - XI Simposio CEA de Bioingeniería*, 179–189. doi:10.4995/CEABioIng.2019.10047.